

This is to certify that the

thesis entitled

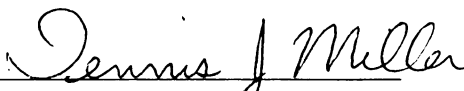
THE RAPID PYROLYSIS OF CELLULOSE
AND THE EFFECT OF K_2CO_3

presented by

Kim, Nak Won

has been accepted towards fulfillment
of the requirements for

M.S. degree in Chemical Engineering


Major professor

Date 5/22/06



RETURNING MATERIALS:
Place in book drop to
remove this checkout from
your record. FINES will
be charged if book is
returned after the date
stamped below.

--	--	--

THE RAPID PYROLYSIS OF CELLULOSE
AND THE EFFECTS OF K_2CO_3

By
Kim, Nak Won

A THESIS

Submitted to
Michigan State University
in partial fulfillment of the requirements
for the degree of

MASTER OF SCIENCE

Department of Chemical Engineering

1986

ABSTRACT

THE RAPID PYROLYSIS OF CELLULOSE AND THE EFFECTS OF K_2CO_3

By

Kim, Nak Won

The rapid cellulose pyrolysis with and without K_2CO_3 has been performed in a heated screen reactor to find the effects of temperature, pressure, and holding time. The electrodes and the shape of screen were modified from earlier experiments to heat a sample rapidly and uniformly, and aluminum foil was used to collect condensed tar.

The tar yield (43 wt %) from pure cellulose pyrolysis at $650^\circ C$ at 15 mm Hg total pressure is much larger than the yield (31 wt %) at $750^\circ C$. The product yields were independent of pressure in the range 10-760 mm Hg.

Rapid pyrolysis with K_2CO_3 as well as slow pyrolysis with other additives resulted in drastically increased char and decreased tar yields. The tar obtained from cellulose pyrolysis was analyzed by G.C. and H.P.L.C. and found to contain levoglucosan, D-glucose, and unknown components. The unknown component at retention time 20 minutes in H.P.L.C. is increased with increasing weight of K_2CO_3 .



To my parents and wife



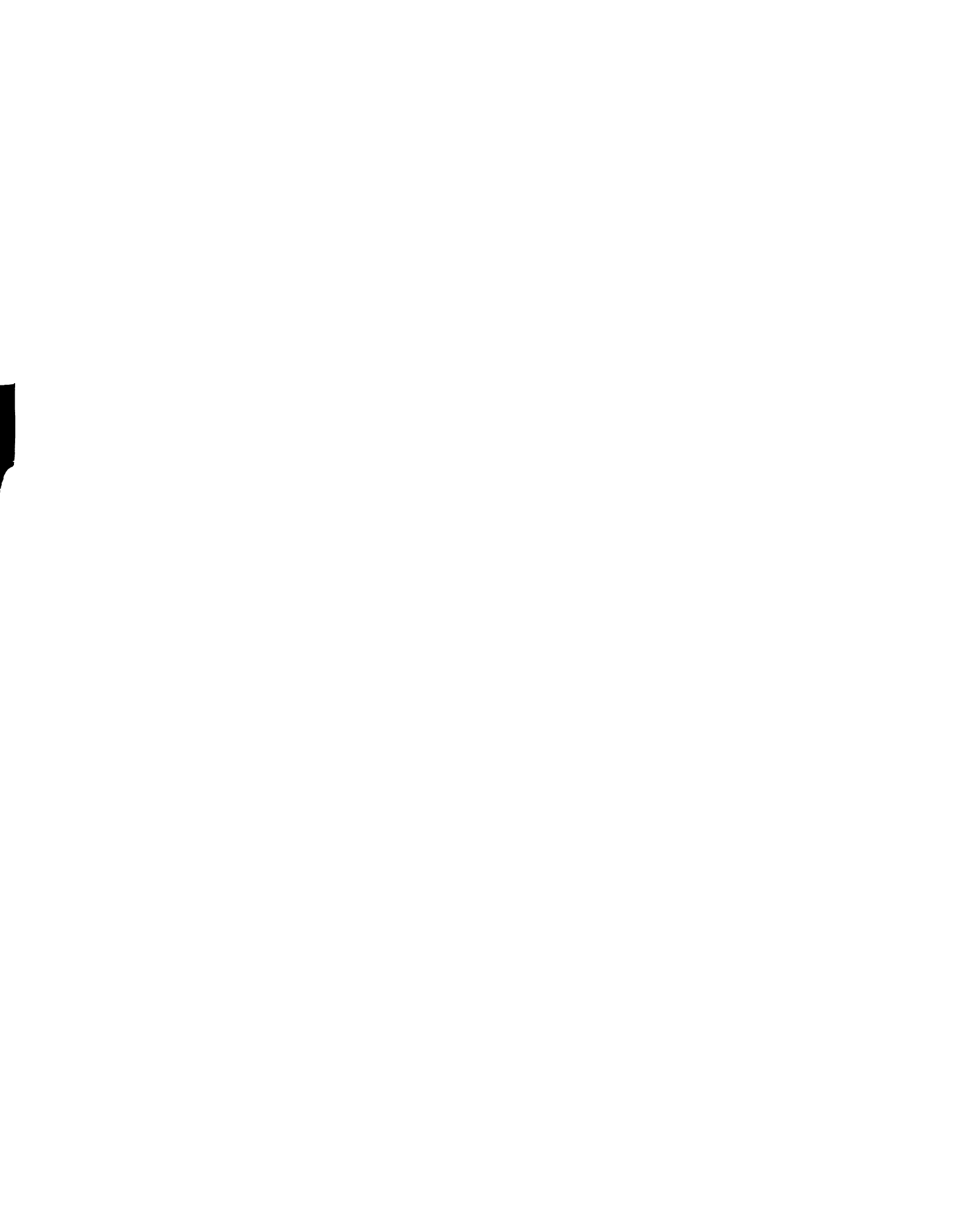
ACKNOWLEDGMENTS

I would like to acknowledge the continuous and indispensable education support provided by Dr. Dennis J. Miller for the completion of this degree.



TABLE OF CONTENTS

	Page
LIST OF TABLES -----	vi
LIST OF FIGURES -----	vii
CHAPTER	
I. INTRODUCTION -----	1
A. The Need for Energy from Biomass -----	1
B. Pyrolysis from Wood -----	3
C. Requirements of Rapid Cellulose Pyrolysis -	6
D. Effects of Impurities in Pyrolysis -----	8
E. Research Objective -----	10
II. EXPERIMENTAL APPARATUS -----	12
A. Pyrolysis Reactor -----	12
B. Electrical System -----	15
C. Gas Collection System -----	21
III. EXPERIMENTAL TECHNIQUE -----	35
A. Cellulose Sample and Foil Preparation -----	35
B. Wire Screen Preparation -----	36
C. Sample Loading -----	37
D. Preparation for Gas Collection and Analysis	37
E. Gas Calibration -----	37
F. Flash Pyrolysis -----	40
G. Collection of Pyrolysis Gas -----	41



CHAPTER	Page
H. Collection of Tar -----	43
I. Analysis of Tar -----	44
J. Collection of Char -----	44
IV. SAMPLE CALCULATION AND EXPERIMENTAL RESULTS ----	46
A. Calculation of Weight of Calibration Gases -	46
B. Calculation of Weight of Pyrolysis Gases ---	47
C. Calculation of Product Composition -----	47
D. Tabulated Data and Calculated Results -----	49
V. DISCUSSION AND CONCLUSIONS -----	65
A. Temperature and Pressure Effects on Pure Cellulose Pyrolysis -----	65
B. Effects of K_2CO_3 -----	67
C. Analysis of Tar -----	69
D. Conclusions -----	74
E. Recommendation -----	75
REFERENCES -----	76
APPENDIX A -----	78
APPENDIX B -----	86
APPENDIX C -----	89

LIST OF TABLES

TABLE	Page
1. Number of Counts for Calibration Gases -----	49
2. Number of Counts of Pyrolysis Gases ----- (CO, CH ₄ , CO ₂ , H ₂)	50
3. Weight of Pyrolysis Gases -----	52
4. Weight Percent of Pyrolysis Gases -----	54
5. Weight and Weight Percent of Char and Tar ---	56
6. Number of Counts of Pyrolysis Gases ----- (C ₂ H ₄ , H ₂ O)	58
7. Weight and Weight Percent of C ₂ H ₄ and H ₂ O ---	60
8. Weight Percent of Pyrolysis Products -----	62
9. Average Weight Percent of Pyrolysis Products at Various Conditions -----	64

LIST OF FIGURES

FIGURE	Page
1. Structure of 3 Components in Wood -----	2
2. Cellulose Degradation -----	4
3. Pyrolysis Reactor -----	14
4. Electrical System of Pyrolysis Reactor -----	17
5. Electrical System of Gas Analysis -----	20
6. Gas Collection System -----	24
7. Sorptometer -----	34
8. Tar Analysis (0 wt % K_2CO_3) -----	70
9. Tar Analysis (5 wt % K_2CO_3) -----	71
10. Tar Analysis (10 wt % K_2CO_3) -----	72
11. Relation between Power and Temperature	
11-a, b, c, d, e, f -----	83
12. Chromatogram of Water Calibration [a, b] ----	87
13. Chromatogram of Pyrolysis Gases -----	90
(CO , CH_4 , CO_2 , H_2 , C_2H_4)	
14. Chromatogram of Pyrolysis Gas (H_2) -----	91
15. Chromatogram of Pyrolysis Gas (H_2O) -----	92

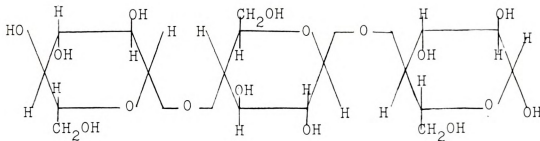
CHAPTER I
INTRODUCTION

A. The Need for Energy from Biomass

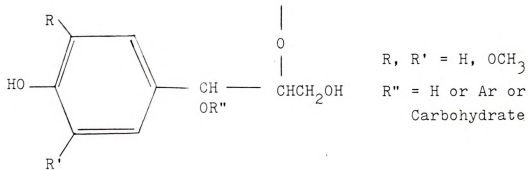
The increasing scarcity of and the rising costs for developing petroleum and natural gas oil stocks have stimulated interests in future sources of these commodities. Changeover to other sources of fuels and chemicals, including coal, oil shale, peat, and tar sands, are possible alternative fossil resources for the near future.

The development of these resources remains an environmental and technical issue and final depletion is ultimately inevitable. However, biomass, another alternative source of energy, is renewable and offers minimal environmental effects because of its low sulfur and nitrogen contents: many types also have very low ash. Therefore, biomass can provide a fraction of total energy requirements or nearly all chemical feedstock needs. A strict definition of the term "biomass" refers to material produced by plants grown on land or in water [1]. In a broader sense, however, biomass is generally defined as the results of direct photosynthesis (terrestrial and aquatic plants) as well as indirect photosynthesis [2]. This definition enables us to include the recurring byproducts of life processes (animal residues) and civilization (municipal solid wastes, sewage, and industrial wastes) [2]. For a country without resources of fossil fuels, these alternative and renewable biomass material can provide feedstocks

= Cellulose =



= Lignin =



= Hemicellulose =

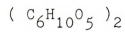
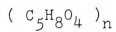


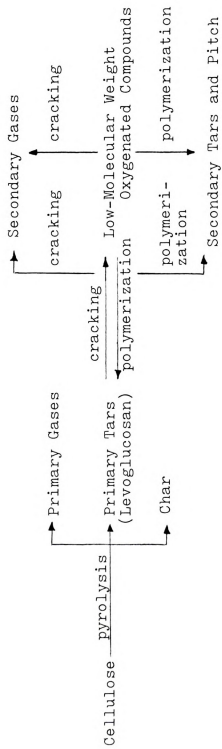
Figure 1. Structure of 3 Components in Wood

for chemical and energy production. An example of such a country which could utilize biomass as fuel is Brazil. But the availability of biomass resources is obviously a function of its management. This management depends on a variety of facts including the cost of fossil-based fuels, chemical and economic climate, and available technology. Unfortunately, its effects are still very uncertain worldwide despite the development of biomass for chemicals, fuels, and energy.

Anyway, it is obvious that biomass utilization for energy is likely in the future. So, as a contribution to biomass technology, research on cellulose pyrolysis has been initiated on the basis of much information related to coal gasification, wood combustion, and fire-proof fibres. Our research in this field emphasizes the effects of process conditions and impurities for rapid, high temperature cellulose pyrolysis.

B. Pyrolysis from Wood

Wood consists of three kinds of components: cellulose, lignin, hemicellulose. It is known that cellulose composes about one-half of wood, and lignin and hemicellulose make up the rest, depending on the tree species. As shown in Figure 1, the structure of each component is quite different: lignin has a quite complex and irregular form. Therefore, in laboratory scale experiments, the consistent structure of model sample of



4

Figure 2. Cellulose Degradation

cellulose is recommended, and is commercially readily available.

Pyrolysis of cellulose, generally in the absence of air in order to minimize the yield of water and CO₂ from oxidation reactions, converts the solid polymeric composite into degradation products that can be in the solid state (char), the liquid state (condensable tar), and the gaseous state. The gas phase contains mostly carbon monoxide, carbon dioxide, and minor proportions of hydrogen, methane, ethene, and other light hydrocarbons.

From a number of experiments, many researchers [3,4] have proposed the pathway of biomass pyrolysis, including cellulose pyrolysis, shown in Figure 2 as an overall simplified mechanism of the process. As shown in Figure 2, the pyrolytic process is composed of many parallel and consecutive reactions that yield different products. In this pathway, gases are produced directly or indirectly by depolymerization (cracking) reactions. Formation of levoglucosan, which is believed to be a principal intermediate compound, takes place at somewhat high temperature (over 280°C) and leads to further decomposition reactions at elevated temperature. It is suggested that the main pyrolysis products of levoglucosan from secondary reactions may be classified as fixed gases such as hydrogen, carbon monoxide, carbon dioxide, methane, acetylene, ethylene and propane, as well as semi-volatiles such as low molecular weight alcohols, ketones, aldehydes, and carbonyl

compounds, aliphatic acids, hydrocarbons, and furan.

Some investigators [6,10,11,13,14] reported the analysis of tar by various methods: Gas Chromatography (GC), Gas Chromatography and Mass Chromatography (GC / MS), Thin-Layer Chromatography (TLC), Liquid Chromatography (LC), and Infrared Spectroscopy. They confirmed that levoglucosan (1,6 anhydro- β -D-glucopyranose) is the main component in tar and that the yield of tar (levoglucosan) depends on the employed conditions which will be described in the next Section.

C. Requirements of Rapid Cellulose Pyrolysis

There are three major products (char, tar, gases) in rapid pyrolysis [4-9,16,17] as well as slow pyrolysis [10-15]. The proportions of each of the three types of products are a function of the condition under which the pyrolysis is carried out.

The most important factor influencing the pyrolysis yield is temperature. A lot of literature has shown the effects of peak temperature on the yields of char, tar, and gases. Hajaligol et al. [8] observed that low temperatures (<600°C) favor tar and char production, with the gas being dominated by water. Intermediate temperatures (700°C) maximize tar production, reduce char production, and augment gas evolution, primarily carbon monoxide. Higher temperatures (750 to 1100°C) significantly increase gas formation via secondary cracking of the tar.

Heating rate, which is another factor influencing the yields of tar, char, and gases for the pyrolysis, is directly connected with peak temperature. At the slow heating rate and high peak temperature, the pyrolysis will take place more slowly and result in secondary cracking at lower temperature. At the rapid heating rate and low peak temperature, the yield of tar will be dominant, as time is not allowed for secondary cracking to occur. Gases constitute the remaining products.

The effect of sample holding time is also explained in various studies [3, 8]. It is generally agreed that holding the sample at the final temperature in low temperature pyrolysis gives continuing decomposition, so that additional tar and gases are made and char yield is decreased. At high temperature, the effects of holding time are negligible for the char yields, but the yield of tar is decreased and the yields of gases are increased, because the formed tar is believed to be decomposed by high temperatures of the screen.

Only a few studies were found which addressed the effect of pressure on pyrolysis [8]. They showed that increasing inert gas pressure in pyrolysis gave decreased yield of tar and increased production of gases. From these results, it is understood that there is not much influence unless significant pressures are exerted during pyrolysis.

Hajaligol et al. [8] observed the effect of sample dimension by using S NO. 507 Filter Paper (101 micrometers

thickness) in the rapid pyrolysis. They showed that increasing the thickness of cellulose decreased the yield of tar and increased yields of the light gases such as hydrogen, methane, propylene, carbon monoxide, ethylene and carbon dioxide.

The effects of inert gas [3] on the pyrolysis can be explained by comparing the effects of oxygen or air. Pyrolysis under oxygen or air is known to result in the fast depolymerization, large carboxyl compounds, carbon monoxide, carbon dioxide, and water. Thus, to minimize water and oxygenated compound production by oxidation reaction, usually oxygen or air is excluded from the pyrolysis.

Another very important factor influencing the proportions of the products for rapid pyrolysis is impurities in the cellulose. This will be explained in Section D.

D. Effect of Impurities in Cellulose Pyrolysis

The pyrolysis of different cotton cellulose [10, 11] with and without flame retardants have been studied to develop better flame retardants. When any kind of biomass burns, the thermal degradation known as pyrolysis occurs and tar (mainly levoglucosan), water, carbon monoxide, carbon dioxide, char, and other inflammable volatile products such as hydrogen and methane are formed. Those volatiles react in the gas phase with atmospheric oxygen and result in a flame. Since it is difficult to prevent

the combustion of these volatiles, many researchers have tried to find the better flame-retardants to prevent their formation.

The major role of the flame retardants is to change the volatiles formed into the non-combustible materials and water vapor. Therefore, the flame retardant may be considered to dehydrate the cellulose. Pictet, Sarasm and Venn pyrolyzed cotton cellulose under reduced pressure and at low temperature (300°C) found that the yield of tar was much greater from purified cotton cellulose than from raw cotton. Besides them, Madorsky et al. [14] fully pyrolyzed, at low temperature in vacuum, samples of cotton and viscous rayon after they had been impregnated with sodium carbonate and with sodium chloride. Madorsky concluded that the salts caused a decrease in the yield of tar and an increase in the yields of residue (char) and gases. Recently, Parks et al. [15] studied the effect of about 50 different impurities on the amounts of char, carbon monoxide, and carbon dioxide produced. In summary, it is generally believed that fire retardant as inorganic compounds and impurities increase the yield of water, carbon monoxide, carbon dioxide, and char, while decreasing the yield of the tar fraction and other inflammable volatile products.

Despite many studies conducted about the effects of the impurity on pyrolysis, there are none for the rapid pyrolysis at high temperature. In this study cellulose with and without potassium carbonate was pyrolyzed under 15

mm Hg and 760 mmHg pressure at 650°C, 750°C set point temperatures. The products from light gases to the components of the tar fraction were analyzed quantitatively using Gas Chromatography and High Performance Liquid Chromatography.

E. Research Objective

As shown in Section D, the pyrolysis of various biomass including cellulose with additives showed the role of those additives at low temperature and slow heating rate: additives increase the yield of char and gases and decrease the yield of tar. Researchers have investigated whether the additives influence mainly cellulose during the primary reaction, or levoglucosan and other degradation products during secondary reactions, since the efficiency of those additives depends on their availability at the appropriate stage or phase of the pyrolysis. They indicate that additives act mainly on cellulose in the solid phase, but they do not rule out the possibility of catalytic interaction with the decomposition products in the vapor phase. The previous experiments using potassium carbonate performed by Jonatan E. Trautz [17] might explain the possibility: he analyzed the remaining char after pyrolysis using neutron activation studies and concluded that 1 wt % K_2CO_3 on cellulose might play a role as catalyst. This is because the potassium carbonate was found in the residual char, but higher percentages of potassium carbonate (5,10

wt %) were lost during the pyrolysis and thus might not be a catalyst. Therefore, as a continuing study, this work emphasizes the formation of tar and its analysis with and without K_2CO_3 on cellulose under 15-760 mm Hg of helium and near $750^{\circ}C$ peak temperature for the rapid pyrolysis.

Recently, some literature [6] have shown that levoglucosan is dominant in the tar analysis after rapid pyrolysis without additives. But nowhere has the tar analysis after rapid pyrolysis with some additives been reported. Whether pyrolysis will give the same tar composition with and without additives is herein investigated.

CHAPTER II
EXPERIMENTAL APPARATUS

The apparatus constructed for the study of the pyrolysis of cellulose at various condition is designed as follows.

A. Reactor

The reactor used in the experiments consists of several main parts: stainless steel tube, ceramic tube, thermocouple, aluminum foils, copper electrodes, copper wire, and screen.

A 6" in length by 2" O.D. stainless steel tube, which is connected to a 1/4" copper tube and swaged to a 2" Swagelock fitting, is made air tight so that it can be run at any pressure. Through a Swagelock connected to a 1/8" copper tube, helium is introduced. The power supply leads are insulated 8 gauge copper wire introduced into the reactor through air tight Conax fittings. These power supply leads connect to the electrodes.

Inside the stainless steel tube is a ceramic tube to insulate the steel tube from electricity and heat and to provide a location on which to wrap the aluminum foil. Aluminum foils are used to collect tar in the reactor during pyrolysis: one of the aluminum foils is installed inside the ceramic tube, and the others are placed on the copper wire and copper electrode, particularly at the



Figure 3. Pyrolysis Reactor

1. Helium Gas Inlet
2. Electric Wire Inlets
3. Thermocouple Inlets
 - a. Thermocouple on the wall
 - b. Thermocouple between the Screen folded in half
4. Brass Cross Fitting
5. 2" Swagelock Fitting
6. Reactor Support
7. Stainless Steel Tube
8. Ceramic Tube
9. Copper Electrode
10. 325 Mesh Wire Screen
11. Gas Outlet

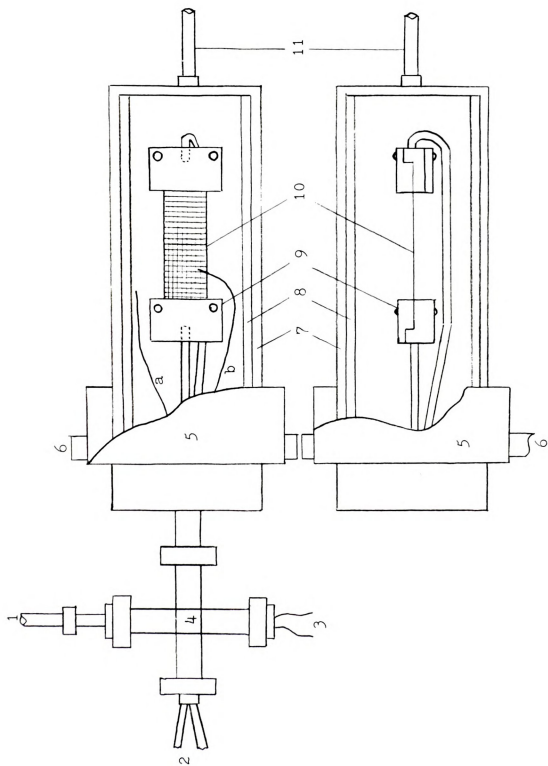


Figure 3. Pyrolysis Reactor

outlet of reactor. Almost all tar after pyrolysis is collected near the outlet of reactor. Since levoglucosan decomposes over 280°C , after pyrolysis almost all levoglucosan is supposed to condense in the reactor.

One of the thermocouples, an ungrounded junction Chromel-Alumel (K) type, is placed near the wall to measure ambient temperature, and the other, an exposed junction Chromel-Alumel (K) type, is placed between the folded 325 mesh stainless steel screen. The exposed Chromel-Alumel thermocouple is connected to the temperature controller which regulates the screen temperature.

The wire screen used in this experiment is folded in half and a small hole is made in which to insert the thermocouple. The sample is placed between the screen which is then stretched between the electrodes. To heat the sample rapidly and uniformly, the copper electrode parts are designed as shown in Figure 3. When the screen is heated, the thin cellulose sample between the screen will be uniformly heated. Therefore, as mentioned in Section C in CHAPTER I, the cellulose sample will be decomposed satisfactorily and reproducibly.

B. Electrical System

The electrical system used in the pyrolysis experiment is drawn in Figure 4 and 5. Figure 4 is the electrical system for the pyrolysis reactor. Figure 5 is the electrical system for the product gas analysis. The pyrolysis

Figure 4. Electrical System of Pyrolysis Reactor

1. Electron Arc Division Power Supply
2. Magnetic Contactor
3. Omega 4001 Single Set Point Proportional
and On-Off Controller
4. Omega Model 650 Thermocouple Thermometer
5. Exposed Junction Chromel-Alumel (K) Type
Thermocouple
6. Ungrounded Junction Chromel-Alumel (K) Type
Thermocouple
7. Copper Electrode
8. 325 Mesh Wire Screen
9. Enlargement of Electrical System inside
Reactor
10. Vacuum Gas Line
11. CENCO-MEGAVAC Vacuum Pump



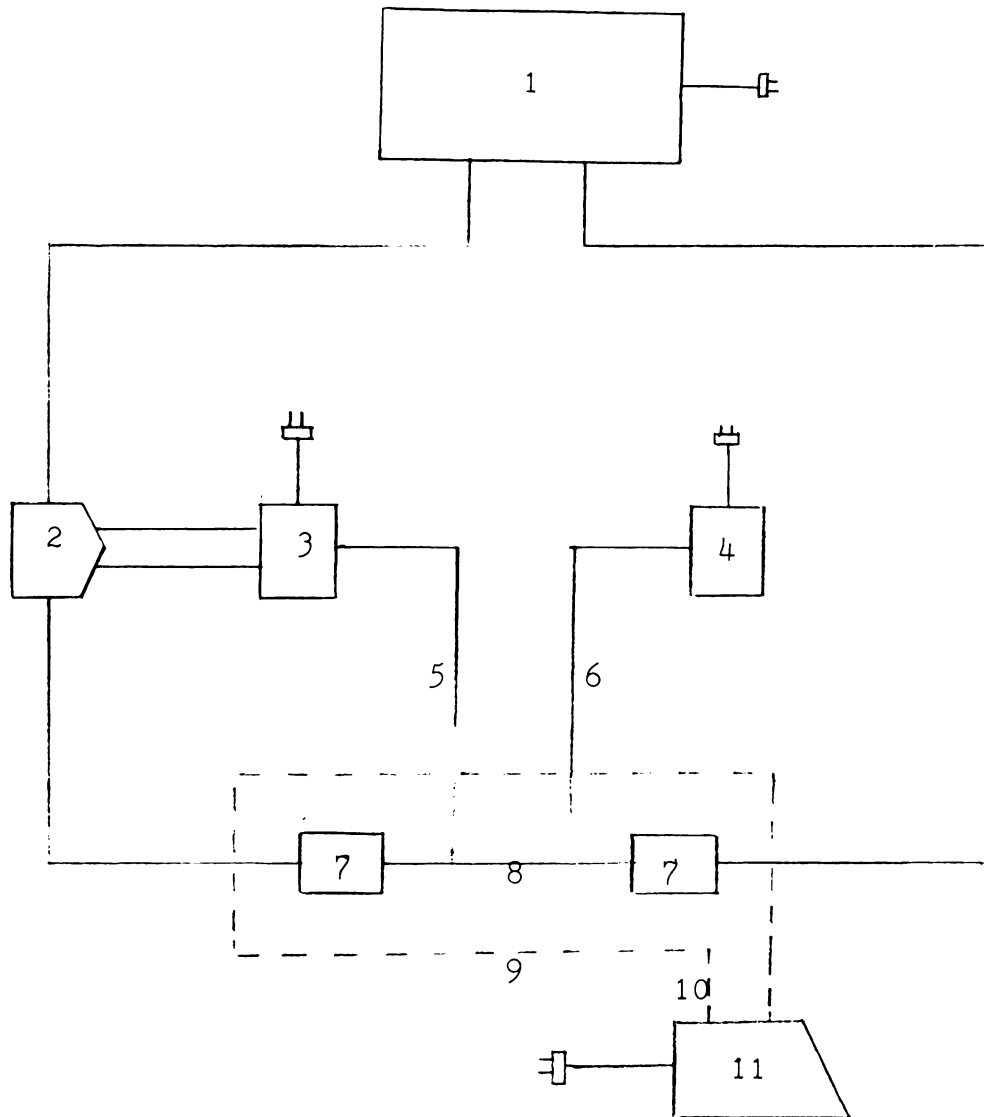


Figure 4. Electrical System of Pyrolysis Reactor

reactor system will be discussed first.

The actual power requirement for rapid pyrolysis ($>200^{\circ}\text{C}$ per second) was determined by repeated experiments, since the difference between the actual and the theoretical power requirement is somewhat large. The theoretical and actual power requirement will be shown in Appendix A.

Figure 4 shows the electrical system for the pyrolysis reactor. The Electron Arc Division Power Supply (1) used in the experiment transfers alternating current into direct current. According to the previous experiments at 200°C per second heating rate, the maximum current was around 36 amperes. The exposed Chromel-Chromel thermocouple (5) placed between the screen is connected to an Omega 4001 Single Set Point Proportional and On-Off Controller (3). The other thermocouple (6), used to measure the ambient temperature, is connected to an Omega Model 650 Thermocouple Thermometer (4). The controller is connected to a Magnetic Contactor (2) which opens the circuit coming from the power supply when the temperature of the screen is above the set point temperature, and closes when the temperature is lower than the set point temperature. Because of the delay in response from the thermocouple, controller, and contactor, the temperature of the screen was found to oscillate around the set point. When the controller was set at 650°C , the highest peak temperature was around $720\text{-}760^{\circ}\text{C}$, and when it was set at 750°C , the highest peak temperature was over 950°C . The results of

Figure 5. Electrical System of Gas Analysis

1. Power/Mate Corporation Power Supply
2. Model 154L Perkin-Elmer Vapor Fractometer
3. Model XKR Sargent-Welch Recorder
4. Sargent-Welch Electronic Integrator
5. 6-Port Valve described in Figure 6
6. Hydrogen Transfer System
7. Omega Model 4001 Single Set Point
Proportional and On-Off Controller
8. Model 40-200 GOW-MAC Power Supply
9. Sorptometer

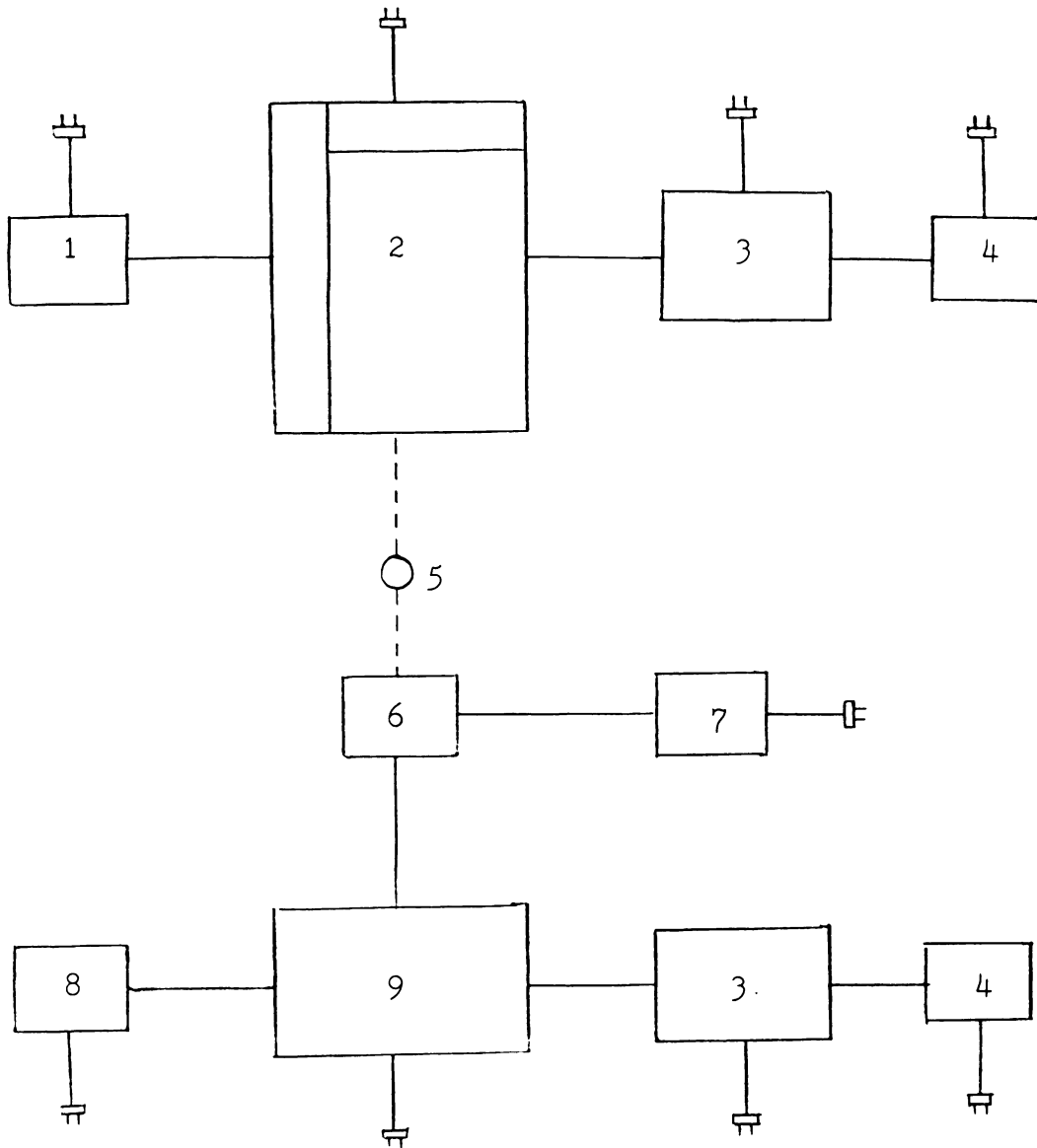


Figure 5. Electrical System of Gas Analysis

pyrolysis at 750°C and at 650°C set temperature will be shown in CHAPTER IV. The outlet of the reactor is connected to the vacuum pump which is connected to 110 volts A.C.

Figure 5 shows the electrical system for the gas analysis. The system is divided into two parts: one for the hydrogen gas analysis, and the other one for other pyrolysis gas (CO, CH₄, CO₂, C₂H₄, and H₂O) analysis. The Model 154L Perkin-Elmer Vapor Fractometer gas chromatograph and the Sorptometer used for gas analysis are equipped with a thermal conductivity detector. The Wheatstone Bridge Circuit system and filaments which compose the detector are used to describe differences in the thermal conductivities of the carrier gas (reference) and the product gases. Therefore, both need a D.C. power supply (1).

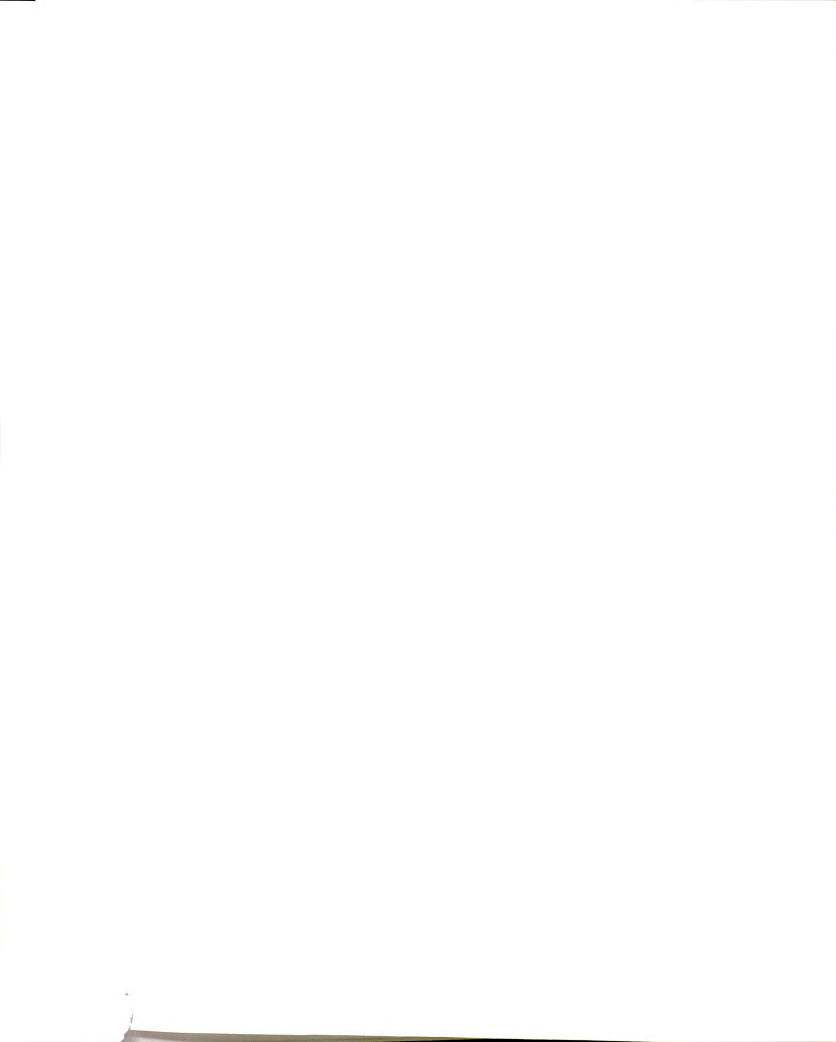
The Fractometer (2) uses 110 volts A.C. power to run the blower fan and heat the column. The electrical signal generated from the Fractometer (2) and the Sorptometer (9) is relayed to the Model XKR Sargent Welch Record (3) with integrator (4). Therefore, the gas analysis can be made quantitatively and qualitatively. An Omega Model 4001 Single Point Proportional and On-Off Controller controls the temperature of the Hydrogen Transfer System (27). The controller is normally set at 500°C.

C. Gas Collection System

A schematic diagram of gas collection system for CO, CH₄, CO₂, H₂O, C₂H₄, and H₂ in the pyrolysis experiments is

Figure 6. Gas Collection System

1. Helium Gas Tank
2. Liquid Nitrogen Trap
3. Whitey Sample Cylinder
4. T-Connector
5. 2-Way Nupro Metering Valve
6. T-Connector and Pressure Gauge
7. Pyrolysis Reactor
8. 3-Way Whitey Ball Valve
9. T-Connector and Vacuum Gauge
10. 2-Way Whitey Ball Valve
11. CENCO-MEGAVAC Vacuum Pump
12. 3-Way Whitey Ball Valve
13. Atmosphere Vent in the G.C. Line
14. Bubble Flow Meter
15. Model 154L Perkin-Elmer Vapor Fractometer
16. 6-Port Valve
17. Dry Ice / Acetone Trap
- 18 and 19. 3-Way Whitey Ball Valve
20. Liquid Nitrogen Trap
21. 6-Way Whitey Valve
22. Sample Loop
23. Calibration Gas Atmosphere Outlet
24. Calibration Gas Tank (CO, CH₄, CO₂)
25. Calibration Gas Tank (H₂)
26. Desiccator
27. Hydrogen Transfer System



28. Thermal Conductivity Detector
29. Bubble Flow Meter
30. Gilmont Gas Rotameter
31. Capillary Tube
32. Fairchild Regulator
33. Nupro Shut Off Valve
34. Particle Filter
35. Molecular Sieve Dryer
36. Nupro Shut Off Valve
37. Nitrogen Tank

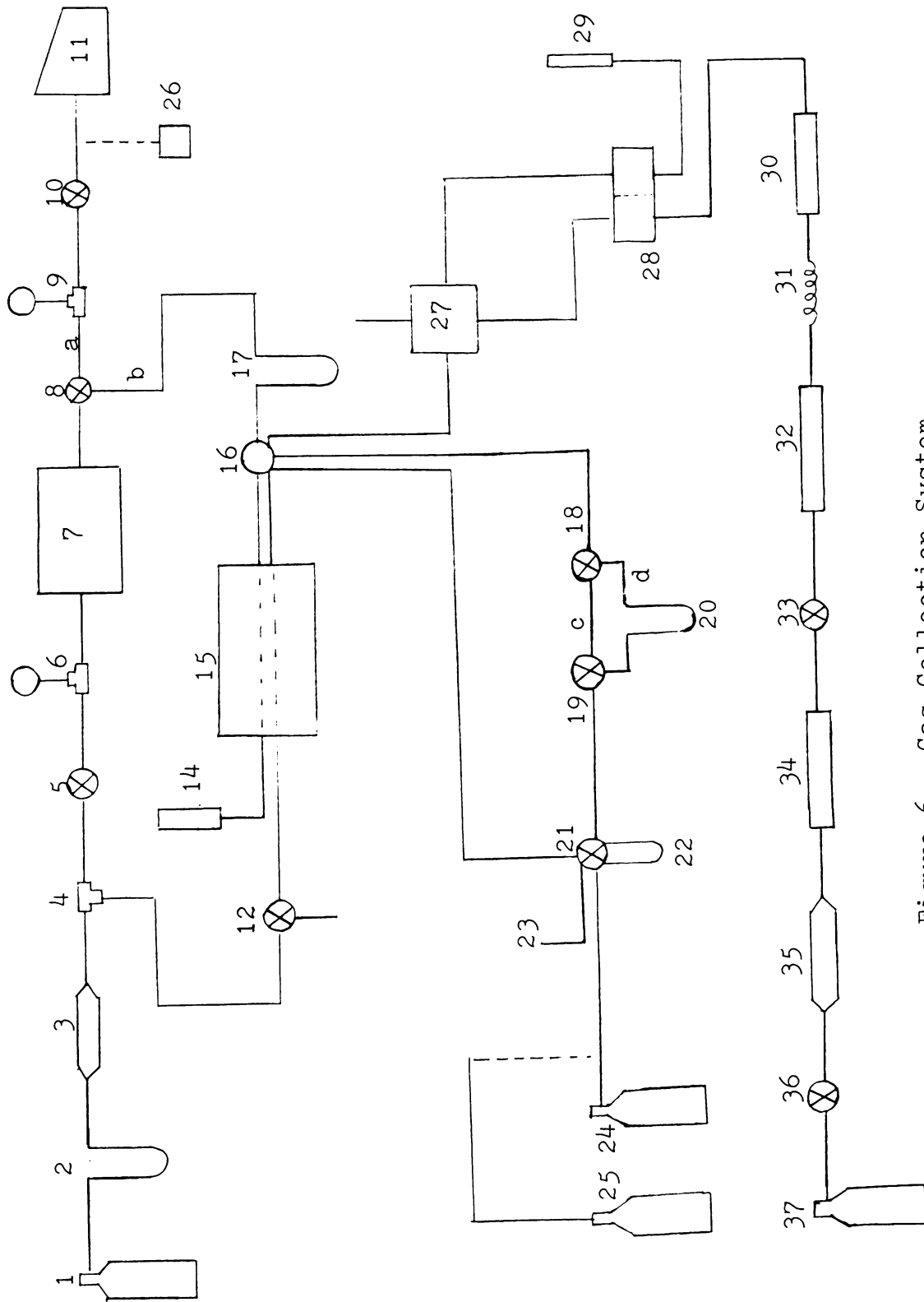


Figure 6. Gas Collection System

shown in Figure 6. The sorptometer shown in Figure 6 as a part of the hydrogen analysis, is also shown in total in Figure 7. In this section, we will discuss the function of the various equipment used in the experiment. The numbers in the parenthesis refer to the equipment shown in Figure 6. Some of these descriptions are taken from J. E. Trautz [17].

(1) Helium Gas Tank : Helium (99.999%) was used as a purge gas in the pyrolysis experiments. As mentioned in Section C in CHAPTER I, helium is used as an inert to minimize oxidation reactions in pyrolysis as well as a carrier gas in the gas chromatograph.

(2) Liquid Nitrogen Trap : This trap consists of a 14" by $\frac{1}{4}$ " O.D. U-shaped stainless steel tube. Inside the tube is 0.5 grams of silica gel desiccant (6-16 mesh) used to absorb impurities which might be in the helium. The U-shaped tube placed under the Dewar flask of liquid nitrogen (-196°C).

(3) Whitey Sample Cylinder : A 500 cc sample cylinder filled with Linde 3A molecular sieves ($\frac{1}{8}$ " pellets) is used to further absorb impurities missed by the upstream nitrogen cold trap. By passing the helium through the liquid nitrogen trap (2) and the sample cylinder, almost all impurities influencing the yields of products from pyrolysis will be removed.

(4) T-Connector : The dried and purified helium is split into two lines: one to the gas chromatograph and the

other to the reactor.

(5) 2-Way Nupro Metering Valve : The valve regulates the helium flow rate through the pyrolysis reactor. For the collection of hydrogen by the Hydrogen Transfer System (27), this valve regulates the lowest helium flow rate that will be more precisely explained at the Hydrogen Transfer System (27).

(6) T-Connector and Pressure Gauge : This gauge is used to detect pressure changes caused by leakage in the reactor before running each sample.

(7) Pyrolysis Reactor : This has been already discussed in detail in the preceding section.

(8) 3-Way Whitey Ball Valve : This valve has three functions. At the "off" position, it is used to check the leakage of the reactor before pyrolysis. One of the "on" position (a) allows gases to pass through the reactor so that the reactor can be evacuated by the vacuum pump (11), when pyrolysis is run at 15 mm Hg helium. This function is also to eliminate air after the cellulose sample is loaded and the reactor is sealed. Another "on" position (b) is used to purge the product gases after pyrolysis from the reactor through two loops, (17) and (20), and to the Hydrogen Transfer System (27).

(9) T-Connector and Vacuum gauge : This gauge is used to measure pressure after evacuation.

(10) 2-Way Whitey Ball Valve : This valve is used to isolate the reactor after evacuation to check for leakage.

(11) CENCO-MEGAVAC Vacuum Pump : This is used to operate the reactor at pressures below one atmosphere. It is also used to evacuate and to eliminate impurities in the reactor before pyrolysis.

(12) 3-Way Whitey Ball Valve : This valve allows helium gas to flow through the G.C. or to be vented to the atmosphere at (13).

(13) Atmosphere Vent in the G.C. Line : This vent is used to vent impurities to the atmosphere when the sample cylinder molecular sieves are being regenerated by heating at 200°F.

(14) Bubble Flow Meter : This is used to determine the flow rate through the G.C. The flow meter is connected to the outlet of the G,C, downstream from the column side of the detector.

(15) Model 154L Perkin-Elmer Vapor Fractometer : This gas chromatograph is used to analyze the product gases from the pyrolysis experiments. The column used in this chromatograph is a 60/80 mesh Carbosieve S-II. The dimensions of this stainless steel column are 5 ft, in length by 1/8" O.D. It was used successfully to separate CO, CH₄, CO₂, C₂H₄, and H₂O.

(16) 6-Port Valve : This valve has two position having three functions. The first position allows the product gases coming from the dry ice / acetone trap (17) to pass through the sample collection loop (20) and to the H.T.S. (27) for selectively analyzing hydrogen. In this

position, gaseous products from the reactor are collected in the sample collection loops, (17) and (20). The helium gas passing through the G.C. is vented out to the atmosphere (14).

The second position allows the reference side helium from the G.C. (15) to pass through the sample collection loop (20) and return to the G.C. (15). In this way the gaseous products collected in the sample collection loop (20) pass through the G.C. for qualitative and quantitative analysis. In this position, the other gas line from the reactor through the dry ice / acetone trap (17) is connected to the H.T.S. (27).

(17) Dry Ice / Acetone Trap ; This trap consists of a 22" in length by 1/4" O.D. U-shaped stainless steel tube with fiberglass packed inside. The tube is placed in a Dewar flask containing dry ice and acetone (-77°C). The purpose of this trap is to collect any moisture (H_2O) or liquid products (propylene, low molecular alcohols) which are the products of the pyrolysis.

(18) and (19) 3-Way Whitey Ball Valve : These two 3-way valves are used in combination for two purposes. In the first position (d), the gases from sample gas tank (24) or from pyrolysis reactor (7) are collected in the liquid nitrogen trap (20). In the second position (c), helium bypasses the trap.

(20) Liquid Nitrogen Trap : This trap consists of a 12" in length by 1/4" O.D. U-shaped stainless steel tube

placed in a Dewar flask filled with the liquid nitrogen. As the product gas from the reactor passes through this cooled tubing, they condense and are retained in this trap. Since the boiling points of CO (-192.0°C), CH_4 (-161.4°C), CO_2 (-78.5°C), C_2H_4 (-103.9°C) are lower than dry ice / acetone (-77°C) but higher than liquid nitrogen (-196°C), the pyrolysis gases (CO, CH_4 , CO_2 , C_2H_4) pass through the dry ice / acetone trap (17) and are condensed in the liquid nitrogen trap (20).

The trap contains 0.1 grams of silica gel to ensure complete collection of light gases (CO, CH_4 , CO_2 , C_2H_4) which have higher boiling point than liquid nitrogen. After all gases are collected in the trap (20), the trap is placed again in boiling water so that the condensed gases become evaporated again. These gases are flushed into the G.C. for analysis.

(21) 6-Way Whitey Sample Valve : This six port valve is used to keep the calibration gas in the known volume of loop (22) and to have it passed through the nitrogen trap (20) for the calibration. Like the six port valve (16), this valve has two positions. The first position allows the gases coming from the calibration gas tank (24) to flow through the 2.045 cc sample loop (22) and to exit to the atmosphere at the calibration gas outlet (23). In the second position, the collected calibration gases are injected to the liquid nitrogen trap (20) by the flow of helium gas, and are eventually analyzed at the G.C. (15)

Those gases are then exited to the atmosphere (14).

(22) Sample Loop : This 36.8" length by 1/8" O.D. tube has a volume of 2.045 cc and is used to measure the volume of calibration gases.

(23) Calibration Gas Atmosphere Outlet : At the step of calibration gas, the gas from the tank (24) or (25) is exited to the atmosphere (23) after passing through 2 cc sample loop (22).

(24) Calibration Gas Tank (CO, CH₄, CO₂) : This tank contains a gas of known composition. The composition by volume is 4.9 percent CO, 4.8 percent CH₄, 4.9 percent CO₂, and helium.

(25) Calibration Gas Tank (H₂) : Pure hydrogen (99.995 percent in volume) was used as a calibration gas.

(26) Desiccator : In order to dry the cellulose sample, the desiccator with sodium hydroxide is used. Also, in the process of tar analysis, it is used to dry the tar solution in the votex tube with the vacuum pump after evaporation with the nitrogen stream.

(27) Hydrogen Transfer System : The basis of the H.T.S. is the transfer of hydrogen from one carrier gas system into a second carrier gas system for measurement. Since hydrogen has non-linear and unpredictable behavior when measured by thermal conductivity in helium carrier, nitrogen gas is chosen as an alternative carrier. The reason that helium is not good as a carrier is because hydrogen has a thermal conductivity just slightly higher

than helium, and would be expected to produce peaks opposite in direction to those produced by other gases. Hydrogen Transfer System consists of two parts: an outer stainless steel chamber and an inner palladium alloy tube. The hydrogen carried in helium from the 6-port valve (16) enters the inner palladium capillary tube of the H.T.S. As the hydrogen moves down the tube, it passes through the selectively permeable wall of the palladium alloy into a nitrogen carrier gas which is flowing in the opposite direction within the annular space formed by the two tubes. Hydrogen passes from the side with the higher partial pressure of hydrogen to the side with the lower partial pressure. Since the nitrogen carrier gas sweeps the hydrogen away to the detector immediately, the direction of hydrogen transfer is always from the helium carrier gas to the nitrogen carrier gas.

(28) Thermal Conductivity Detector : The difference between the thermal conductivities of the carrier gas (nitrogen) and the components of interest (hydrogen) is detected in the detector cell using thermistor filaments.

(29) Bubble Flow Meter : This is used to determine the flow rates of helium and nitrogen, respectively. The flow rate of helium is measured when the 6-port valve (16) is turned to the "Reactor through Loop" position.

(30) Gilmont Gas Rotameter : This rotameter is used for measuring flow rate of nitrogen.

(31) Capillary Tubing : This tube is 6 ft. in length

and 1/16" O.D.

(32) Fairchild Mode 10112V Regulator : This is used to control the pressure of nitrogen carrier gas in the sorptometer.

(33) and (36) Shut Off Valve : A Nupro Shut Off Valve is used to control the flow rate of nitrogen.

(34) Particle Filter : After passing through the Molecular Sieve Dryer, the nitrogen passes through this filter to further absorb impurities.

(35) Molecular Sieve Dryer : Like the Whitey Sample Cylinder (3), this is used to absorb impurities including moisture.

(37) Nitrogen Tank : Nitrogen (99.998%) is used as a carrier gas in the Hydrogen Transfer System (27). In the previous explanation of the H.T.S. (27), the utility and selectivity of nitrogen for the hydrogen analysis was illustrated.



Figure 7. Sorptometer

1. Thermal Conductivity Detector
2. Bubble Flow Meter
3. Sample Cell
4. Exit atmosphere
5. Valco Valve
6. Flow Meter
7. Control Valve
8. Liquid Nitrogen Trap
9. Dampener
10. Nitrogen Tank
11. Regulator
12. NuproShut Off Valve
13. Molecular Sieve Dryer
14. Particle Filter
15. Nupro Shut Off Valve
16. Fairchild Pneumatic Pressure Regulator
17. Moor Pressure Gauge
18. Capillary Tubing
19. Gilmont Gas Rotameter
20. Helium Tank



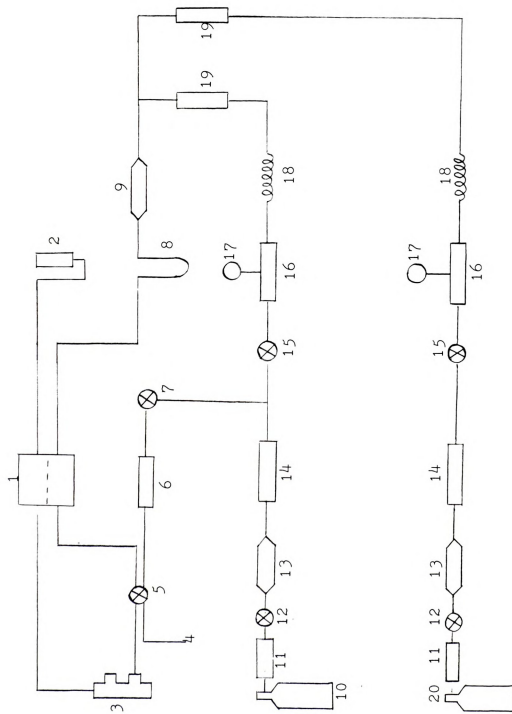


Figure 7. Sorptometer



CHAPTER III

EXPERIMENTAL TECHNIQUE

This chapter shows the procedure of the experiments in detail. The order of the sections in this chapter corresponds to that in the actual experiments. The numbers and letters in parentheses refer to the equipment and directions shown in Figure 6 in CHAPTER II, respectively.

A. Cellulose Sample Preparation

To study the effects of impurities in cellulose during the rapid pyrolysis, two kinds of samples are prepared: one is pure cellulose and the other is cellulose treated with K_2CO_3 .

The pure cellulose used in the experiments is # 4 Whatman filter paper. Since the ash in the cellulose can act as a catalyst, low ash content filter paper (0.06 percent by weight) is chosen in this experiment. Also the thickness of the filter paper (0.008 inch) is such that heat penetration is effective and therefore the sample temperature is uniform during pyrolysis.

The samples were prepared with 0, 5, and 10 weight percent K_2CO_3 in cellulose. Samples were placed in the desiccator at least for one week after preparation to dry entirely. The dried sample was cut and weighed to 14 mg. After that, the weighed sample is kept in the desiccator to prevent absorption of moisture.



B. Wire Screen and Foil Preparation

Aluminum foils are prepared to collect the tar in the reactor. There are three foils used to collect the tar in the reactor : these are placed inside the ceramic tube wall, on the electrode, and on the copper wire. The foils are first cut to size, then cleaned with acetone to eliminate unknown impurities, and weighed.

The wire screen used in the experiment is 325 mesh stainless steel screen. The screen is cut to 4 by 8 cm. and folded in half. A small hole is made to put the thermocouple in the screen. The screen is placed through the electrodes without thermocouple and then heated at the set point temperature for 10-20 seconds to remove impurities.

The preheated screen is then weighed and placed through the electrode tightly. The advantages of the tightly stretched screen are explained in Section A in CHAPTER II. The thermocouple is cleaned with acetone to remove any tar which may be presented from the previous experiments. The uncleaned tar can give higher yield of gases by secondary reactions as shown in CHAPTER I.

Finally, the screen is heated again with thermocouple to confirm the heating rate and to eliminate impurities which might be on the screen. The foils are then placed in the proper locations.

C. Sample Loading

The prepared cellulose sample is loaded between the folded screen. After loading the sample, the reactor is sealed with 2" Swagelock Fitting and the product gas outlet is connected.

The biggest problem in this batch type reactor is the leakage of air. As shown in CHAPTER I, the thermal degradation under air or oxygen has a different kinetic route and is undesirable. Moreover, elevated gas pressure in the reactor after pyrolysis at 1 atmosphere causes pyrolysis gas to leak unless the reactor is sealed completely. To test for leakage, the reactor is pressurized to 40 psig. If no change is found in pressure after 30 minutes, the vacuum pump (11) is switched on, the 2-Way Whitey Ball Valve (10) is changed to the "on" position, and the 3-Way Whitey Ball Valve (8) is switched to route (a). In this step, the pressurized helium gas is vented and air in the reactor is eliminated. After 5 minutes, the 3-Way Whitey Ball Valve (8) is changed to the "off" position and the reactor is pressurized to 1 atmosphere pressure with helium. After that, the 3-Way Whitey Ball Valve (8) is switched again to route (b).

D. Preparation for Gas Collection and Analysis

The column pressure controller in the gas chromatograph is set to 14 psig and the column flow rate is established at 30 cc per minute using bubble flow meter



(14) and regulating the column pressure controller. Both power / Mate Corporation Power Supply (1) in Figure 5 and the detector voltage switch on the G.C. are turned to the "on" position and adjusted to 9 volts. The recorder and integrator are turned on and fixed at attenuation 32 and chart speed 2 cm per minute. The G.C. temperature controller is turned to the blower setting which activates the oven fan.

In order to purify the column in the G.C. (15) and the three traps (2), (17), (20) which may have collected impurities during the previous experiments, boiling water is placed around each trap, and the 6-Port Valve (16) is turned to the "G.C. through Loop" position. The G.C. temperature controller is turned to 220°C and the column is heated. After the column temperature arrives at 220°C, boiling water around the trap (2) is replaced by liquid nitrogen to capture impurities in the helium carrier gas. Boiling water around the trap (20) is removed and the 3-Way Whitey Ball Valves (18) and (19) are changed to route (c) to keep the loop (20) clean. After the trap returns to room temperature, the trap (20) is placed in liquid nitrogen for 5 minutes before injection of the calibration gases (CO, CH₄, CO₂). In this step, zero adjustment is made by regulating the zero point of the Sargent-Welch Recorder. Now the gas collection system is ready to be used.

E. Gas Calibration

With the gas collection system ready, the 6-Way Whitey Valve (21) is turned to allow calibration gas to flow through the sample loop (22). The calibration gas from the tank (24), which has 4.9, 4.8, 4.9, volume percent of CO, CH₄, CO₂, respectively, flows through 2.045 cc copper loop (22) and is vented to the atmosphere (23). After purging the calibration gases from the tank (24) into the sample loop (22) for 1-2 minutes, the 3-Way Whitey Ball Valves (18) and (19) are switched to route (d) to flow gas through the trap (20). The 6-Way Whitey Ball Valve (21) is switched to inject calibration gas into the helium stream flowing through the trap (20). The 3-Way Whitey Ball Valves (18) and (19) are changed to route (c) to isolate the collected gases in the loop (20). The Model XKR Sargent-Welch Recorder and Integrator are adjusted to the "pen" position.

To analyze the calibration gas, after boiling water is placed around the trap (20) and the 3-Way Whitey Ball Valves (18) and (19) are switched so helium gas flushes the gases to the chromatograph, the Model XKR Sargent-Welch Recorder and Integrator are adjusted to the "record" position. The temperature controller on the G.C. is turned to 175°C after 2 minutes. After arriving at 175°C, the temperature controller is turned to blower position to cool down the column, and the 3-Way Whitey Ball Valves (18) and (19) are changed to route (c) to keep the loop (20) clean.

The Hydrogen Transfer System is calibrated according



to the following procedure. Analysis of hydrogen requires nitrogen carrier gas, because the thermal conductivities of hydrogen and helium are so close that analysis is difficult. In the sorptometer, the nitrogen gas from the tank (37) comes out by opening the Nupro Shut Off Valve (36). Impurities in nitrogen gas are removed at the Molecular Sieve Dryer (35) and at Particle Filter (34). The flow rate of the filtered nitrogen gas is controlled at 30 cc per minute by the Fairchild Pneumatic Pressure Regulator (32). The flow rate is checked by the gas rotameter (30) and bubble flow meter (29).

Hydrogen calibration (99.995% in volume) is passed through 2.045 cc copper loop (22) and vented to the atmosphere (23) for 1-2 minutes. To inject hydrogen for calibration, the 6-Port Valve (16) is switched to the "Reactor through Loop" position, and the 6-Way Whitey Ball Valve (21) is switched to inject hydrogen through route (c) of the loop (20) to the H.T.S. (27). Several pulses of hydrogen are used to clean the instrument.

F. Flash Pyrolysis

After the calibration gas analysis, the dry ice/acetone trap (17), liquid nitrogen trap (20), and G.C. column do not have to be cleaned again. To run flash pyrolysis at 15 mm Hg with helium, the reactor must be evacuated. Therefore, after the 2-Way Nupro Metering Valve (5) is closed and the 3-Way Whitey Ball Valve (8) is opened



to the vacuum pump (11), the vaciim pump (11) is operated for 5 minutes. The 2-Way Whitey Ball Valve (10) is then closed and the pressure in the reactor is regulated to 15 mm Hg with helium using 2-Way Nupro Metering Valve (5) and pressure gauge (9). The 3-Way Whitey Ball Valve (8) is changed to close position. Before pyrolysis, the trap (17) is placed in the dry ice / acetone bath, and the trap (20) is placed in liquid nitrogen bath to collect pyrolysis gases during the purging step after pyrolysis.

Pyrolysis experiments were run at two set point temperature (650°C and 750°C) and in two modes: one where the heater was shut off immediately after the peak temperature was reached, and another where the peak temperature was maintained for about twelve seconds. As mentioned earlier, the delay in response from the thermocouple, controller, and contactor caused the actual thermocouple temperature to overshoot by 100°C at 650°C and 200°C at 750°C . The temperature of the screen oscillated around the set point in the extended experiments.

G. Collection of Pyrolsis Gases

After pyrolysis, the reactor is cooled down to room temperature to condense the tar sufficiently. After 5-10 minutes, the reactor is pressurized to one atmosphere with helium by regulating 2-way Nupro Metering Valve (5). The **Sargent-Welch** Recorder and Integrator are prepared to analyze hydrogen by connecting the output leads from the



sorptometer to the recorder. The attenuation on the power supply is changed to 64 and 6-Port Valve (16) is switched to "Reactor through Loop" (17), (20), and the flow rate of purge gas is adjusted to 30 [cc / minute] so that the fraction of hydrogen recovered is maximized. Analyzing the hydrogen gas component takes about 40 minutes and the peak of hydrogen comes out at 3.3-3.6 minutes. During this flushing step, the other gases, CO, CH₄, CO₂, C₂H₄, and H₂O are collected in the traps (20) and (17).

Following hydrogen analysis, gases collected in the traps are analyzed by G.C. The recorder and integrator are prepared for analysis of these gases by adjusting the zero point with the G.C. zero knob while the column is at room temperature. To analyze the gases, the trap (20) is removed from liquid nitrogen, while the dry ice / acetone bath is kept around the trap (17) to hold product. Boiling water is placed around the trap (20) and the XKR Sargent-Welch Recorder is switched to the "record" position. Simultaneously, the 3-Way Whitey Ball Valves (18) and (19) are turned to allow helium to flow through the trap. After 2 minutes, the temperature controller on the G.C. is turned to 175°C. In this operation, the peak for each product appeared at 2.8-3.1 minutes for CO, at 5.7 minutes for CH₄, at 8.3 minutes for CO₂, at 14.6 minutes for H₂O, and at 16.5 minutes for C₂H₄. The typical chromatogram will be shown in Appendix B. When the temperature in the G.C. column arrives at 175°C, the temperature controller on the



G.C. is switched to the blower position to cool the column.

The components in the dry ice / acetone trap (17) are next analyzed. Boiling water around the trap (20) is removed and the 3-Way Whitey Ball Valves (18) and (19) are turned to route (c). After 5 minutes, liquid nitrogen is placed around the trap (20) and the 3-Way Whitey Ball Valves (18) and (19) are changed to route (d). The 6-Port Valve (16) is changed to the "Reactor through Loop" position and boiling water is substituted for dry ice / acetone around the trap (17) to transfer contents (almost all water) of dry ice / acetone trap to the liquid nitrogen trap (20). After 30 minutes, the 3-Way Whitey Ball Valves (18) and (19) are changed to route (c). Boiling water is substituted for liquid nitrogen after adjusting the zero of the recorder. After the recorder is switched to the "record" position, the 3-Way Whitey Ball Valves (18) and (19) are turned to route (d). In the same way as before, after 2 minutes, the temperature controller on the G.C. is switched to 175°C. The peak of H₂O appears at 12.6 minutes and slowly decays for 14 minutes.

H. Collection of Tar

After the quantitative and qualitative gas analysis, the reactor is opened and the tar collected on the three aluminum foils is recovered using rubber gloves to prevent contamination from bare hands. The tar with aluminum foil is weighed and then stored in a vial for future analysis.

The weight of tar is calculated as the difference of foils after and before pyrolysis. Most of tar was collected from the ceramic tube.

I. Collection of Char

In the same way as collection of tar, char is recovered after gas analysis. The char remaining between the folded screen is weighed. Since the char sometimes can not be separated from the screen, the weight of char is measured by the difference of the weight of the screen and the weight including char and screen.

J. Analysis of Tar

Analysis of tar was done using Gas Chromatography and High Performance Liquid Chromatography. In order to separate the tar components in the G.C., the tar on the aluminum foil is trimethylsilylated.

First, the solution of pyridine, trimethylchlorosilane, and hexamethyldisilazane, is made in the ratio 10 to 1 to 1. The solution is then sealed. Some part of the tar collected on the aluminum foil is dissolved with 250 microliter distilled water: the tar solution is then pipetted into a votex tube. The solution is evaporated to dryness under a stream of nitrogen and residue is further dried for more than 2 hours in a vacuum desiccator prior to trimethylsilylation.

For trimethylsilylation, dried tar dissolved with



the three mixed reagents. To dissolve the tar and to activate the reaction, the mixture is stirred vigorously for 0.5-1 minutes. After that, accurately measured aliquots of about 5 microliter are drawn into a 10 microliter Hamilton Syringe and injected into a Varian 3700 Gas Chromatograph equipped with Flame Ionization Detector. The column used is 2 m in length by 1/8" O.D. stainless steel column with packing 3 % OV - 101 on Chromosorb W - HP; the temperature is programmed from 100°C to 230°C at 5°C per minute heating rate. Injector temperature is fixed at 150°C and the ionization temperature is controlled at 280°C.



CHAPTER IV

SAMPLE CALCULATIONS AND EXPERIMENTAL RESULTS

The experimental data for calibration gases, pyrolysis gases, char, and tar, were collected according to procedures in CHAPTER III. This chapter illustrates how those data are manipulated to give the final experimental results.

A. Calculation of Weight of Calibration Gases

The sample gas tank (24) consists of 4.9 %, 4.8 % CH_4 , 4.9 % CO_2 by volume in helium. Hydrogen from tank (25) is 99.995 volume percent pure. A 2045 cc copper loop is used to calibrate for CO , CH_4 , CO_2 , and H_2 , and a 0.056 cc loop is used for C_2H_4 .

Assuming the sample gases are ideal, the weight of each component is calculated by correcting to room temperature in terms of the ideal gas law.

$$\begin{array}{l} \text{Weight} \\ \text{of} \\ \text{Interest} \end{array} = \frac{P \times V \times T' \times 1 \text{ [mole]} \times \text{Molecular wt [gram]}}{P' \times 22400 \text{ [cc]} \times 1 \text{ [mole]}} \quad (4-1)$$

The recorder chart speed is used 2 [cm / minute] for all experiment. Table 1 shows the number of counts for the calibration gases (CO , CH_4 , CO_2 , and H_2) at each run. Since the calibration of H_2O and C_2H_4 is difficult, the fixed values for H_2O and C_2H_4 are used for all experiments.



B. Calculation of Weight of Pyrolysis Gases

Table 2 and 6 shows the number of counts proportional to the peak area of pyrolysis gases (CO , CH_4 , CO_2 , H_2 , C_2H_4 , H_2O) from the experiments. Since the attenuations of calibration (32) for CO , CH_4 , CO_2 , C_2H_4 , and H_2 are the same as pyrolysis experiments, the weight of gases produced (CO , CH_4 , CO_2 , C_2H_4 , H_2O) can be calculated by following Eq. (4-2).

$$\text{Weight of Pyrolysis Gas} = \frac{\text{Weight of Calibration Gas by Eq. (4-1)} \times \text{Number of Counts of Pyrolysis Gas}}{\text{Number of Counts of Calibration Gas}} \quad (4-2)$$

The weight of H_2 is one-sixteenth of the value by Eq. (4-2) since the attenuation of calibration (64) is sixteen times of pyrolysis experiment (4). Table 3 and 7 shows the weight of pyrolysis gases.

C. Calculation of Product Composition

The weight percent of each product from pyrolysis is based on the weight of pure cellulose and is defined as follows:

$$\text{Weight Percent of Product} = \frac{\text{Weight of Pyrolysis Component}}{\text{Weight of Cellulose}} \times 100 \quad (4-3)$$

As a reference, the weight percent of K_2CO_3 is defined as follows:



$$\text{Weight Percent of } K_2CO_3 = \frac{\text{wt. of } K_2CO_3 * 100}{\text{wt. of Cellulose} + \text{wt. of } K_2CO_3} \quad (4-4)$$

Therefore, the weight of cellulose is

$$\text{wt. of Cellulose} = \text{wt. of Sample} * (100 - \text{wt } \% K_2CO_3) \quad (4-5)$$

Table 4 shows the calculated values of weight percent for CO, CH₄, CO₂, H₂, and Tabel 7 for C₂H₄ and H₂O.

Table 5 gives the calculated value of weight and weght percent of tar and char.

D. Tabulated Data and Calculated Results

Table 1. Number of Counts for Calibration Gases

# run	Number of Counts			
	CO	CH ₄	CO ₂	H ₂
1	23.08	20.60	27.20	148.80
2	25.41	22.13	27.60	128.25
3	23.44	22.96	27.88	144.70
4	25.15	23.00	27.51	146.74
5	22.00	19.58	25.45	154.74
6, 7	23.24	20.99	26.99	154.74
8-11,13, 15-17	22.77	19.95	26.94	134.39
12, 14,	23.00	24.50	28.50	141.75
18-20	22.77	19.95	26.94	134.39
21	23.61	21.55	26.55	151.00
22	20.85	20.05	23.84	151.00
23-32	23.75	21.20	30.50	139.18
33	31.70	31.80	32.70	149.88
34-36	23.52	20.87	29.28	148.74
37-39	24.16	23.68	30.68	138.45
40	24.18	21.90	27.60	138.43
41	22.45	21.45	30.76	145.61
42	23.60	21.74	30.49	140.15



Table 2. Number of Counts of Pyrolysis Gases

# run	T [°C]	P [mmHg]	K ₂ CO ₃ wt %	Number of Counts			
				CO	CH ₄	CO ₂	H ₂
1	750	760	0	468.91	72.88	107.34	3286.11
2				477.44	79.76	92.25	-
3				350.74	45.73	75.41	1368.75
4				554.65	104.08	108.50	3974.50
5	750	760	1	346.05	54.25	172.03	2305.06
6				363.44	58.66	167.54	2374.78
7				451.25	83.66	178.10	2803.03
8				438.80	81.16	176.99	2931.08
9	750	760	5	373.83	54.15	261.88	4203.19
10				520.74	78.05	232.67	5534.78
11				446.15	52.60	237.44	4960.43
12				-	-	-	-
13				535.38	65.20	223.50	7167.88
14	750	760	10	573.78	71.17	237.67	7822.90
15				616.40	65.24	191.23	7193.51
16				679.59	66.84	233.42	8912.00
17				556.45	70.45	240.00	7444.93
18	750	10	0	359.95	39.39	66.00	2395.70
19				514.10	61.90	93.85	5229.78
20				522.06	51.76	91.75	3912.60
21				306.70	75.60	100.00	-
22				469.38	53.00	81.81	4168.50
23	750	15	0	-	44.00	88.90	2233.90
24				396.50	43.80	84.88	2331.00
25				472.90	37.20	89.00	3015.75
26				446.79	31.65	84.43	2252.67
27				1371.50	24.60	71.50	286.50
28				-	32.30	80.30	818.00
29				397.90	36.35	77.00	2121.25
30				452.10	41.80	86.00	2415.25
31				-	25.40	91.80	486.10
32				518.38	9.60	88.65	1183.50
33	750	500	0	488.56	77.38	103.33	3127.50
34	650	15	0	307.07	13.70	81.27	2051.13
35				350.08	8.19	78.88	1832.58
36				339.00	11.29	76.74	2175.48
37				300.15	10.00	97.90	1324.50
38				348.26	11.79	110.07	2430.00
39				347.10	17.42	95.30	1546.35
40	650	15	5	327.50	24.40	215.00	3438.89



# run	T [°C]	P [mmHg]	K ₂ CO ₃ wt %	Number of Counts			
				CO	CH ₄	CO ₂	H ₂
41	650	15	5	314.43	20.34	210.05	2268.30
42				-	25.37	-	1516.13
43				-	21.43	225.26	2564.05
44				342.83	21.96	246.93	2502.77
45				299.66	19.59	187.87	2068.88
46				348.34	19.14	211.68	2045.02

The symbol (-) indicates that the components was not analyzed.



Table 3. Weight of Pyrolysis Gases

# run	Weight of Gases [grams]			
	CO ($\times 10^{-3}$)	CH ₄ ($\times 10^{-5}$)	CO ₂ ($\times 10^{-4}$)	H ₂ ($\times 10^{-4}$)
1	2.331	22.724	7.116	2.309
2	2.156	23.150	6.027	-
3	1.717	12.793	4.877	0.989
4	2.531	29.066	7.112	2.832
5	1.808	17.797	12.189	1.557
6	1.795	17.951	11.193	1.624
7	2.228	25.601	11.899	1.894
8	2.211	26.131	11.847	2.280
9	1.884	17.434	17.529	3.270
10	2.625	25.129	15.574	4.305
11	2.248	16.935	15.893	3.859
12	-	-	-	-
13	2.671	17.094	14.141	5.286
14	2.862	18.659	15.035	5.769
15	3.075	17.104	12.099	5.305
16	3.390	17.524	14/769	6.673
17	2.776	18.470	15.185	5.491
18	1.643	10.998	4.326	1.707
19	2.346	17.287	6.152	3.621
20	2.382	14.455	6.014	2.709
21	2.949	22.533	6.792	-
22	2.583	16.979	6.188	2.886
23	-	13.331	5.256	1.678
24	1.916	13.271	5.018	1.751
25	2.285	11.171	5.262	2.265
26	2.159	9.588	4.991	1.692
27	-	7.453	4.227	0.215
28	-	9.786	4.747	0.614
29	1.874	11.013	4.552	1.593
30	2.184	12.665	5.085	1.814
31	-	7.696	5.428	0.366
32	1.104	2.909	5.241	0.890
33	1.769	15.628	5.698	2.181
34	1.498	4.216	5.005	1.449
35	1.708	2.521	4.858	1.288
36	1.654	3.475	4.726	1.529
37	1.426	2.740	5.754	1.000
38	1.654	3.198	6.469	1.835
39	1.649	4.725	5.601	1.168

# run	Weight of Gases [grams]			
	CO (x 10 ⁻³)	CH ₄ (x 10 ⁻⁵)	CO ₂ (x 10 ⁻⁴)	H ₂ (x 10 ⁻⁴)
40	1.554	7.156	14.047	2.597
41	1.607	6.091	12.313	1.629
42	-	7.496	14.336	1.131
43	-	6.332	13.322	1.913
44	1.667	6.488	14.604	1.867
45	1.457	5.788	11.111	1.543
46	1.694	5.655	12.519	1.525

The symbol (-) indicates that the component was not analyzed.

Table 4. Weight Percent of Pyrolysis Gases

# run	Weight [grams]			Weight Percent [wt %]		
	K_2CO_3 ($\times 10^{-4}$)	Cellulose	CO	CH_4	CO_2	H_2
1	0	0.0145	16.08	1.57	4.91	1.59
2		0.0145	14.87	1.60	4.16	-
3		0.0145	11.84	0.88	3.36	0.68
4		0.0146	17.33	1.99	4.87	1.94
5	1.682	0.0143	12.64	1.24	8.52	1.09
6		0.0143	12.55	1.26	7.83	1.12
7	1.311	0.0144	15.47	1.78	8.26	1.32
8		0.0144	15.36	1.81	8.23	1.58
9	9.665	0.0136	13.85	1.28	12.89	2.40
10	9.599	0.0135	19.44	1.86	11.54	2.19
11	9.918	0.0135	16.65	1.25	11.77	2.86
12		0.0135	-	-	-	-
13	9.599	0.0135	19.99	1.55	11.08	4.13
14	18.415	0.0127	22.54	1.47	11.84	4.54
15		0.0127	24.46	1.65	10.08	4.41
16		0.0127	26.96	1.69	12.30	5.46
17	18.230	0.0126	22.26	1.80	12.74	4.60
18	0	0.0141	11.65	0.78	3.07	1.21
19		0.0146	16.07	1.18	4.21	2.55
20		0.0146	16.42	0.99	4.12	1.91
21		0.0145	10.34	1.55	4.68	-
22		0.0146	17.69	1.16	4.24	1.98
23	0	0.0141	-	0.95	3.73	1.19
24		0.0141	13.59	0.94	3.56	1.24
25		0.0141	16.20	0.80	3.72	1.62
26		0.0141	15.31	0.68	3.54	1.20
27		0.0140	-	0.53	3.02	0.15
28		0.0140	-	0.70	3.39	0.44
29		0.0140	13.39	0.79	3.25	1.14
30		0.0140	15.60	0.90	3.62	1.30
31		0.0137	-	0.56	3.96	0.27
32		0.0140	17.89	0.21	3.74	0.63
33	0	0.0147	12.03	1.06	3.88	1.48
34	0	0.0136	11.01	0.31	3.68	1.06
35		0.0140	12.20	0.18	3.47	0.92
36		0.0139	11.90	0.25	3.40	1.10
37		0.0137	10.40	0.20	4.20	0.73
38		0.0139	11.90	0.23	4.68	1.32
39		0.0139	11.86	0.34	4.03	0.84

# run	Weight [grams]			Weight Percent [wt %]		
	K_2CO_3 ($\times 10^{-4}$)	Cellulose	CO	CH_4	CO_2	H_2
40	6.5458	0.0133	11.73	0.54	10.60	1.96
41	6.5932	0.0132	12.10	0.46	9.30	1.23
42	6.5458	0.0132	-	0.57	10.90	0.86
43	6.5659	0.0132	-	0.48	10.10	1.45
44	6.5932	0.0132	12.59	0.49	11.03	1.41
45	6.4035	0.0129	11.33	0.45	8.64	1.20
46	6.5458	0.0132	12.88	0.43	9.52	1.16

The symbol (-) indicates that the component was not analyzed.



Table 5. Weight and Weight Percent of Char and Tar

# run	Weight Percent	Weight [grams]		Weight	Percent
	K ₂ CO ₃	Char	Tar	Char	Tar
1		0.0006	0.0044	4.14	30.34
2	0	0.0005	0.0045	4.14	31.03
3		0.0007	0.0048	4.83	33.10
4		0.0006	0.0045	4.11	31.03
5	1	0.0013	0.0037	9.07	25.82
6		0.0015	0.0038	10.47	26.51
7		0.0014	0.0021	9.74	14.61
8		0.0013	0.0028	9.05	19.49
9	5	0.0028	0.0025	20.54	18.34
10		0.0024	0.0025	17.73	18.46
11		0.0024	0.0020	17.77	14.81
12		0.0019	0.0016	24.37	11.84
13		0.0033	0.0028	24.37	20.68
14	10	0.0033	0.0030	26.07	23.70
15		0.0031	0.0029	24.49	22.91
16		0.0028	0.0031	22.12	24.49
17		0.0038	0.0034	30.21	27.03
18	0	0.0005	0.0050	3.55	35.46
19		0.0004	0.0042	2.74	28.77
20		0.0002	0.0054	1.37	37.00
21		0.0006	0.0044	4.11	30.14
22		0.0006	0.0044	4.11	30.14
23	0	-	0.0042	-	29.79
24		-	0.0051	-	36.17
25		0.0004	0.0045	2.84	31.91
26		0.0002	0.0042	1.42	29.79
27		0.0001	0.0064	0.71	45.71
28		0.0002	0.0051	1.43	36.43
29		0.0001	0.0048	0.71	34.04
30		0.0001	0.0043	0.71	30.71
31		0.0000	0.0052	0.00	37.96
32		-	-	-	-
33	0	0.0090	0.0042	6.12	28.57
34	0	0.0003	0.0059	2.21	43.38
35		0.0003	0.0049	2.14	35.00
36		0.0002	0.0061	1.44	43.88
37		0.0004	0.0060	2.92	43.80
38		0.0003	0.0060	2.16	43.17
39		0.0004	0.0066	2.88	47.48



# RUN	Weight Percent K_2CO_3	Weight Char	[grams] Tar	Weight Char	Percent Tar
40	5	0.0033	0.0020	25.10	15.21
41		0.0037	0.0023	27.95	17.37
42		0.0032	0.0027	24.33	18.25
43		0.0037	0.0022	28.05	16.68
44		0.0036	0.0088	27.19	17.49
45		0.0034	0.0027	26.44	21.00
46		0.0036	0.0024	27.38	18.25

The symbol (-) indicates that the component was not analyzed.



Table 6. Number of Counts of Pyrolysis Gases (C_2H_4 , H_2O)

# run	Weight Percent	Number of Counts	
	K_2CO_3	C_2H_4	H_2O
1	0	46.29	332.43
2		28.52	344.20
3		14.04	207.21
4		37.05	318.11
5	1	17.14	399.59
6		20.28	419.88
7		28.78	315.35
8		30.75	292.75
9	5	12.25	-
10		19.18	225.64
11		-	-
12		-	-
13		11.38	226.80
14	10	7.98	171.17
15		6.24	216.00
16		8.00	179.35
17		11.30	328.15
18	0	13.35	262.05
19		15.10	258.85
20		27.35	279.50
21		-	-
22		17.26	295.89
23	0	37.40	114.05
24		37.00	162.08
25		35.55	245.95
26		34.41	-
27		20.20	193.10
28		30.10	216.30
29		33.60	226.60
30		34.80	194.40
31		25.20	177.80
32		11.25	134.20
33	0	25.58	363.59
34	0	7.58	162.39
35		11.60	190.34
36		14.98	115.24
37		11.91	122.74
38		7.85	217.34
39		17.60	235.64

# run	Weight Percent		Number og Counts	
	K_2CO_3		C_2H_4	H_2O
40	5		4.85	242.39
41			0.87	270.05
42			4.75	297.95
43			3.16	255.04
44			3.78	111.74
45			4.00	338.09
46			3.00	149.28

The symbol (-) indicates that the component was not analyzed.



Table 7. Weight and Weight Percent for C_2H_4 and H_2O

# run	Weight [grams]		Weight Percent	
	C_2H_4 ($\times 10^{-5}$)	H_2O ($\times 10^{-4}$)	C_2H_4	H_2O
1	24.2427	18.7814	1.67	12.95
2	14.9605	19.4463	1.03	13.41
3	7.3648	11.7068	0.51	8.07
4	19.4349	17.9726	1.33	12.31
5	8.9910	22.5757	0.63	15.79
6	10.6381	23.7220	0.74	16.59
7	15.0968	17.8263	1.05	12.37
8	16.1302	16.5395	1.12	11.49
9	6.4259	-	0.47	-
10	10.0611	12.7480	0.75	9.44
11	-	-	-	-
12	-	-	-	-
13	5.9695	12.8136	0.44	9.49
14	4.1860	9.6706	0.33	7.61
15	3.2733	12.2033	0.26	9.61
16	4.1965	10.1328	0.33	7.98
17	5.9275	18.5395	0.47	14.71
18	7.0029	14.8051	0.50	10.50
19	7.9290	14.6243	0.54	10.02
20	14.3467	15.7910	0.98	10.82
21	-	-	-	-
22	9.0520	16.7170	0.62	11.45
23	19.6186	6.4435	1.40	4.57
24	19.4087	9.1571	1.38	6.49
25	18.6481	13.8955	1.32	9.85
26	18.0480	-	1.28	-
27	10.5961	10.9096	0.76	7.79
28	15.7893	12.2316	1.13	8.74
29	17.6252	12.7853	1.26	9.13
30	18.2547	10.9831	1.30	7.85
31	13.2189	10.0452	0.96	7.33
32	5.9013	7.5819	0.42	5.42
33	13.4182	20.5418	0.92	13.97
34	4.1834	9.1746	0.31	6.75
35	6.0849	10.7537	0.43	7.68
36	7.8579	6.5107	0.57	4.68
37	6.2475	6.9345	0.56	5.06
38	4.1178	12.2791	0.30	8.83
39	9.2323	13.3130	0.66	9.58

# run	Weight [grams]		Weight Percent	
	C_2H_4 ($\times 10^{-5}$)	H_2O ($\times 10^{-4}$)	C_2H_4	H_2O
40	2.5441	13.6944	0.19	10.41
41	0.4524	15.2571	0.03	11.52
42	2.4917	16.8333	0.19	12.80
43	1.6589	14.4090	0.13	10.92
44	1.9802	6.3130	0.15	4.77
45	2.0982	19.1011	0.16	14.85
46	1.5737	8.4336	0.12	6.41

The symbol (-) indicates that the component was not analyzed.

Table 8. Weight Percent of Pyrolysis Products

# run	Weight Percent Based on the Weight of Pure Cellulose							
	CO	CH ₄	CO ₂	H ₂	C ₂ H ₄	H ₂ O	Char	Tar
1	16.08	1.57	4.91	1.59	1.67	12.95	4.14	30.34
2	14.87	1.87	4.16	-	1.03	13.41	4.14	31.03
3	11.84	0.88	3.36	0.68	0.51	8.07	4.83	33.10
4	17.33	1.99	4.87	1.94	1.33	12.31	4.11	31.03
5	12.64	1.24	8.52	1.09	0.63	15.79	9.07	
6	12.55	1.26	7.83	1.12	0.74	16.59	10.47	26.51
7	15.47	1.78	8.26	1.32	1.05	12.37	9.74	14.61
8	15.36	1.81	8.23	1.58	1.12	11.49	9.05	19.49
9	13.85	1.28	12.89	2.40	0.47	-	20.54	18.34
10	19.44	1.86	11.54	3.19	0.75	9.44	17.73	18.46
11	16.65	1.25	11.77	2.86	-	-	17.77	14.81
12	-	-	-	-	-	-	14.07	11.84
13	19.99	1.55	11.08	4.13	0.44	9.49	24.37	20.68
14	22.54	1.47	11.84	4.54	0.33	7.61	26.07	23.70
15	24.41	1.65	10.08	4.41	0.26	9.61	24.49	22.91
16	26.96	1.69	12.30	5.46	0.33	7.98	22.12	24.49
17	22.23	1.87	12.75	4.66	0.47	14.71	30.21	27.03
18	11.65	0.78	3.07	1.21	0.50	10.50	3.55	35.46
19	16.07	1.18	4.21	2.55	0.54	10.02	2.74	28.77
20	16.31	0.99	4.12	1.91	0.98	10.82	1.37	37.00
21	10.34	1.55	4.68	-	-	-	4.83	23.45
22	17.69	1.16	4.24	1.98	0.62	11.45	4.11	30.14
23	-	0.95	3.73	1.19	1.40	4.57	2.75	29.79
24	13.59	0.94	3.56	1.24	1.38	6.49	3.28	36.17
25	16.20	0.80	3.73	1.61	1.32	9.85	2.84	31.91
26	15.31	0.68	3.54	1.20	1.28	-	1.42	29.79
27	-	0.53	3.02	0.15	0.76	7.79	0.71	45.71
28	-	0.70	3.39	0.44	1.13	8.74	1.43	36.43
29	13.39	0.79	3.25	1.14	1.26	9.13	0.71	34.04
30	15.60	0.90	3.63	1.30	1.30	7.85	0.71	30.71
31	-	0.56	3.96	0.27	0.96	7.33	0.00	37.96
32	17.89	0.21	3.74	0.63	0.42	5.42	-	-
33	12.03	1.06	3.88	1.48	0.91	13.97	6.12	28.57
34	11.01	0.31	3.68	1.06	0.31	6.75	2.21	43.38
35	12.20	0.18	3.47	0.92	0.43	7.68	2.14	35.00
36	11.90	0.25	3.40	1.10	0.57	4.68	1.44	43.88
37	10.40	0.20	4.20	0.73	0.56	5.06	2.92	43.80
38	11.90	0.23	4.68	1.32	0.30	8.83	2.16	43.17
39	11.86	0.34	4.03	0.84	0.66	9.58	2.88	47.48

# run	Weight Percent Based on the Weight of Pure Cellulose							
	CO	CH ₄	CO ₂	H ₂	C ₂ H ₄	H ₂ O	Char	Tar
40	11.73	0.54	10.60	1.96	0.19	10.41	25.10	15.21
41	12.10	0.46	9.30	1.23	0.03	11.52	27.95	17.37
42	-	0.57	10.90	0.86	0.19	12.80	24.33	18.25
43	-	0.48	10.10	1.45	0.13	10.92	28.05	16.68
44	12.59	0.49	11.03	1.41	0.15	4.77	27.19	17.49
45	11.33	0.45	8.64	1.20	0.16	14.85	26.44	21.00
46	12.88	0.43	9.52	1.16	0.12	6.41	27.38	18.25

The symbol (-) indicates that the component was not analyzed.

Table 9. Average Weight Percent of Pyrolysis Products at Various Conditions

Set Point [$^{\circ}$ C]		750				650			
Temperature									
Pressure [mm Hg]		760		10	15	15			
Avg. of run #	1 2 4	5 7 8	10 13	14 15 16	19 22	23, 24 27-29 31	34 36-38	42, 43 45, 46	
wt % K_2CO_3	10	5	1	0	0	0	0	5	
CO	23.91	19.72	14.49	16.09	16.88	15.70	11.30	12.14	
CH ₄	1.66	1.71	1.61	1.72	1.17	1.79	0.25	0.50	
CO ₂	17.34	11.31	8.34	4.65	4.23	3.63	3.99	10.31	
H ₂	4.54	3.66	1.33	1.77	2.27	1.37	1.05	1.53	
C ₂ H ₄	0.35	0.60	0.93	1.34	0.58	1.30	0.44	0.12	
H ₂ O	10.64	9.47	13.22	12.89	10.74	8.85	6.33	8.90	
Char	26.92	21.05	9.29	4.13	3.43	1.66	2.18	26.75	
Tar	24.55	19.57	19.98	30.80	29.46	30.80	43.56	16.69	

CHAPTER V

CONCLUSIONS AND DISCUSSION

The results of the rapid cellulose pyrolysis with and without K_2CO_3 under various conditions were shown in Table 9 in CHAPTER IV. Those results indicated the effect of temperature and pressure on rapid cellulose pyrolysis, and what the role of K_2CO_3 was. This chapter gives an analysis based on those results.

Table 9 represents the data at two different set point temperatures ($650^\circ C$, $750^\circ C$). It is generally agreed that the tar yield is maximized at some critical temperature near $750^\circ C$. Therefore, the experiments focused on obtaining the maximum yield of tar by setting the temperature controller to $650^\circ C$. When the temperature controller was set at $650^\circ C$ and $750^\circ C$, the highest peak temperatures were around $720-760^\circ C$ and over $950^\circ C$, respectively. The experiments were run at three different pressures of helium (760 mm Hg, 10 mm Hg, 15 mm Hg). The experiments at 760 mm Hg and 19 mm Hg helium were done for 12 seconds duration time, while those at 15 mm Hg helium at both $750^\circ C$ and $650^\circ C$ were run only until the initial peak temperature was reached.

A. Temperature and Pressure Effects on Pure Cellulose Pyrolysis

It is generally believed that temperature and holding

time of rapid pyrolysis are the factors most influencing the pyrolysis product composition. The results of pure cellulose pyrolysis in Table 9 show the effects of temperature.

When the results of pure cellulose pyrolysis at 750°C and 15 mm Hg pressure are compared with those at 650°C and 15 mm Hg pressure, the yield of tar at 650°C (43 wt %) is much larger than the one at 750°C (30 wt %), while the yields of gas and char at 650°C are a little less than those at 750°C. The results are interpreted that the tar formed is decomposed to gases via secondary reactions at elevated temperature. It is generally agreed that secondary cracking of tar increases the yields of carbon monoxide, carbon dioxide, hydrogen and hydrocarbon gases such as CH_4 and C_2H_4 . Hajaligol et al. [8] showed the maximum yield of tar in rapid cellulose pyrolysis occurred at 700°C and gradually decreased at higher temperature. Though the yield of tar in this experiment is less than theirs [8], the results are generally in agreement. The lower tar yield possibly results from loss of volatile liquids during purging.

The effects on pressure in cellulose pyrolysis at 750°C are negligible, as the yields at 760 mm Hg and 10 mm Hg showed no difference at all. Therefore, the effects of pressure on cellulose pyrolysis at high temperature are not important unless possibly the pressure is increased to a very large value.

The results of pyrolysis at 750°C and 10 mm Hg and 15 mm Hg pressure in Table 9 show the effects of holding time. Only slight differences are found in product composition, indicating that almost all intermediate vaporized products diffuse out of the cellulose and the pyrolysis is complete when the peak temperature is reached. Therefore, it can be concluded that the yields of products for very thin cellulose pyrolysis at rapid heating rate (>200°C per second) and at high peak temperature (>950°C) are not dependent on holding time at the peak temperature.

B. Effects of Impurities (K_2CO_3)

The literature [10-15] shows the effects of additives on products from slow pyrolysis. These results conclude that the role of additives in pyrolysis is to reduce the yield of tar while increasing the yields of char, CO, CO₂, and H₂O. Though these results are from slow pyrolysis, results from our experiments indicate the same trends.

From the comparison of pure cellulose pyrolysis with K₂CO₃-treated cellulose pyrolysis, it is confirmed that K₂CO₃ increases the char yield and decreases the tar yield drastically regardless of the set point temperature. At 750°C set point temperature and 760 mm Hg pressure, the results of four different samples (0, 1, 5, and 10 weight percent K₂CO₃ cellulose samples) are shown in Table 9. As the weight percent of K₂CO₃ on the cellulose sample is increased, the yields of CO, CO₂, and H₂ show a monotonic



increase, while the yields of hydrocarbons (CH_4 , C_2H_4) are reduced. Moreover, the yield of char is drastically increased while the yield of tar was abruptly decreased. The CO yields from the 1 wt % K_2CO_3 samples are scattered, perhaps as a result of nitrogen impurity during the gas chromatographic analysis. Nevertheless, the yield of CO shows a gradual increase with increasing K_2CO_3 . When the results of 5 wt % K_2CO_3 cellulose pyrolysis are compared at two different set point temperature (650°C , 750°C), it is found that gases and char yields at 750°C are larger than those at 650°C , while the tar yield at 750°C is smaller than that at 650°C . Even though the comparison is somewhat difficult because the actual weight percent of K_2CO_3 for the sample at 750°C is a little larger than the one at 650°C , the results could be explained by the relationship between the presence of K_2CO_3 on the cellulose and the temperature of the screen. It is generally agreed that the yield of tar is maximized around 750°C , that the yield of char is increased at lower temperature, and that K_2CO_3 as a flame retardant lowers the activation energy and threshold temperature of the pyrolysis. These facts explain the results in light of the higher rate of volatilization at lower temperatures and the increased yield of the residual char, which lessens the flaming combustion [3].

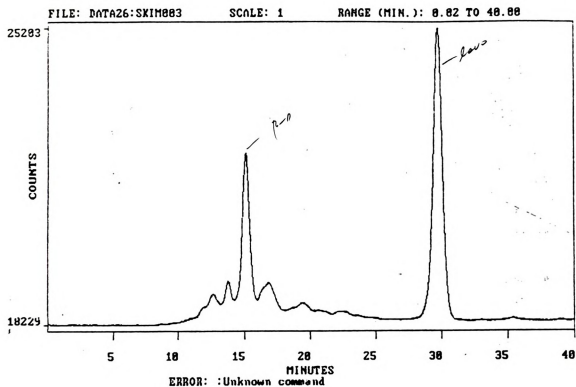
Therefore, the analysis of the products suggests that K_2CO_3 primarily promote the dehydration and charring of

cellulose, and lessen the cleavage of intact pyranose monomers (as levoglucosan). This is in agreement with Madorsky et al. [14], who proposed in 1956 that sodium chloride and sodium carbonate as additives catalyze the dehydration of cellulose by scission of the C-O bond and thus increase the yield of CO, CO₂, H₂O, and char at the expense of levoglucosan. This proposal seems to be valid for the interpretation of these results (Table 9) of K₂CO₃ loaded cellulose in rapid pyrolysis.

C. Analysis of Tar

Figures 8, 9, and 10 show the results of analysis of tar obtained from the 0, 5, and 10 weight percent K₂CO₃ loaded cellulose in rapid pyrolysis. The tar analysis was done by High Performance Liquid Chromatography [19] and by Gas Chromatography [18]. Since the results of tar analysis by G.C. showed only the presence of levoglucosan and D-glucosa, the results by H.P.L.C. only are shown in this chapter. The only calibrated components in the analysis were D-glucose and levoglucosan: therefore, the analysis focuses on the composition ratio for each tar sample.

Figure 8 shows that levoglucosan and D-glucose are dominant components in tar analysis for pure cellulose pyrolysis. The ratio of levoglucosan to glucose is more than 2 to 1. The peaks at retention time 15.1 minutes and 29.7 minutes are D-glucose and levoglucosan, respectively. The peaks at retention time 12.6 and 13.7 minutes are



```

=====
                          AREA PERCENT REPORT
=====

```

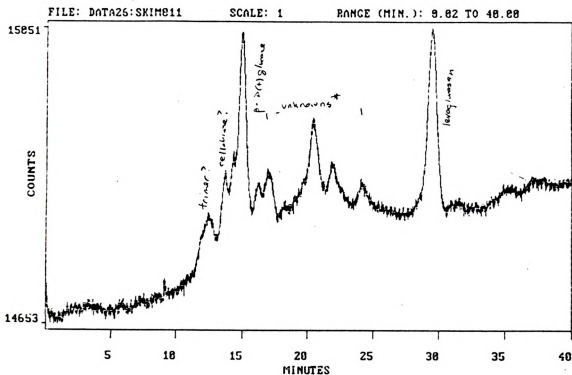
Peak	R.T. (min)	Area Percent	Area	Peak Ht	BL
1	12.642	3.761	19095	366	BV
2	13.767	2.716	13789	515	VB
3	15.101	24.882	126324	3447	BB
4	16.785	0.646	3281	28	BB
5	22.055	0.558	2834	36	BB
6	29.722	67.437	342379	6828	BB
TOTAL		100.000	507702		

```

=====

```

Figure 8. Tar Analysis (0 wt % K_2CO_3)

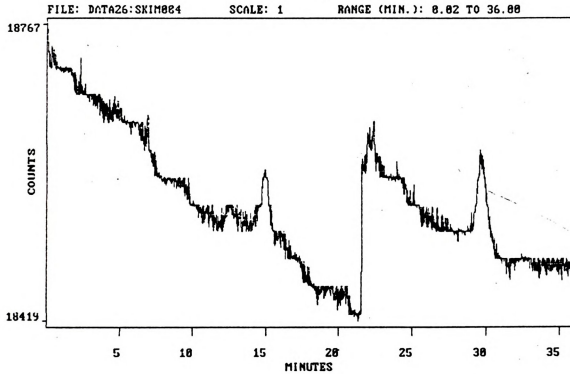


```

=====
                          AREA PERCENT REPORT
=====
Peak   R.T.(min)   Area Percent   Area   Peak Ht   BL
-----
   1    14.950    32.865       7934    225     VB
   2    20.432    12.613       3045     82     BB
   3    29.500    54.521      13162    250     BB
-----
TOTAL                                100.000   24141
=====

```

Figure 9. Tar Analysis (5 wt % K_2CO_3)



```

=====
                          AREA PERCENT REPORT
=====
Peak   R.T.(min)   Area Percent   Area   Peak Ht   BL
-----
  1     21.867     60.203        3269   134       BV
  2     22.150     39.797        2161   122       VV
-----
TOTAL                100.000      5430
=====

```

Figure 10. Tar Analysis (10 wt % K_2CO_3)

postulated to be dimers and cellulbiose, but no confirmation is possible.

Figure 9, which is the tar analysis of 5 weight percent K_2CO_3 cellulose sample, represents somewhat similar results to Figure 8, but it is seen that the area ratio of levoglucosan and D-glucose is decreases to around 1.7 to 1, while the yield of the unknown product at a retention time 20.4 minutes is drastically increased. Also in this experiment, the amounts of levoglucosan and D-glucose were about one-twenty sixth and one-sixteenth respectively of those for pure cellulose, even though the amount of tar analyzed was within a factor of two of the pure cellulose.

Figure 10, which is the tar analysis of the cellulose pyrolysis with 10 weight percent of K_2CO_3 , shows similar results. It is very difficult to interpret each peak except levoglucosan and D-glucose.

Some literature [6,13] has shown levoglucosan is the main component in tar in slow pyrolysis as well as in rapid cellulose pyrolysis. But the quantity of levoglucosan in tar depends on temperature, heating rate, residence time, additives, molecule structure, and even crystallinity. Therefore, it can be concluded from these figures that the amount of levoglucosan in tar decreases as the weighy of K_2CO_3 on cellulose is increased, while some unknown components are drastically increased.

D. Conclusions

The gaseous products of rapid cellulose pyrolysis with and without K_2CO_3 at high temperature were quantitatively analyzed by Gas Chromatography and char and tar yields were measured by weighing. The rapid pure cellulose pyrolysis at high temperature resulted in more tar yield and less char yield as the temperature on the screen was increased up to $750^\circ C$. Some secondary cracking of levoglucosan occurred at higher temperature. When K_2CO_3 -treated cellulose was pyrolyzed at the same conditions (temperature, pressure, heating rate), the yield of tar was drastically decreased and char yield was increased. In addition, the yields of CO and CO_2 were increased, while the yields of hydrocarbons (CH_4 , C_2H_4) were slightly decreased. In the tar analysis, it was confirmed that levoglucosan is dominant component in tar for pure cellulose pyrolysis, but as the amount of K_2CO_3 was increased, the quantity of levoglucosan in the tar decreased and the yield of the unknown components in tar increased. Therefore, the presence of K_2CO_3 in rapid cellulose pyrolysis as well as in slow pyrolysis has a catalytic effects on dehydration and bond scission, and alters the pyrolytic mechanism to yield more char, CO, CO_2 , H_2O , H_2 , and other components in tar.

E. Recommendation

Although the contour of the influence of additives

and the predominance of levoglucosan in tar in pyrolysis experiments has been manifested, it still remains to identify the unknown components and to manifest the reason why they are increased with increasing the additives.

To yield more tar and other products (low molecular alcohol, furfuran, etc.), it is suggested to modify the reactor. In this experiment, aluminum foils were used to collect the condensed tar, so that some of tar and other products which have low boiling points did not condense on the foils and thus were lost. Thus, to spray water with high pressure might be more effective to collect volatile products without loss before the temperature in the reactor reaches at room temperature. This modified reactor, however, might require more complex equipment and procedure: water sprayer, liquid collector, heating tape, etc.

LIST OF REFERENCES



LIST OF REFERENCES

- [1] T. A. McClure, E. S. Lipinsky, "Handbook of Biosolar Resources" Vol. II (1981)
- [2] I. S. Goldstein, presented in Symposium on Alternate Feedstocks for Petrochemicals, 18th Nat. Meet. Amer. Soc., Las Vegas, Nev (1980), Abstract PETR 21
- [3] F. Shafizadeh, "Pyrolysis and Combustion of Cellulose Materials", Advances in Carbohydrate Chemistry, 23, pp. 419-475 (1968)
- [4] P. C. Lewellen, W. A. Peters, J. B. Howard, "Cellulose Pyrolysis Kinetics and Char Formation Mechanism" Sixteenth Symposium (International) on Combustion, The Combustion Institute Pittsburg, pp. 1471-1479 (1977)
- [5] Toshimi Hirata, "Pyrolysis of Cellulose, An Introduction to the Literature", U. S. Department of Commerce, NBSIR 85-3218, August (1985)
- [6] C. I. DeJenga, M. J. Antal Jr., "Yields and composition of Sirups Resulting from the Flash Pyrolysis of Cellulosic Materials Using Radiant Energy", Journal of Applied Polymer Science, Vol. 27, pp 4313-4322 (1982)
- [7] J. Diebold and J. Scahill, "Ablative Fast Pyrolysis of Biomass in the Entrained-Flow Cyclonic Reactor" at S.E.R.I., Fourteenth Biomass Thermochemical Conversion Contractors Meeting, Arlington, Virginia June 23-24, (1982) U. S. Department of Energy Contract # DE-AC06-76RLO 1830
- [8] M. R. Hajjaligol, W. A. Peters, J. B. Howard and J. P. Longwell, "Product Compositions and Kinetics for Rapid Pyrolysis of Cellulose", Ind. Eng. Chem. Prod. Res. Dev., 21 (1982)
- [9] X. Deglise, C. Richard, A. Rolin and H. Francois, "Fast Pyrolysis/Gasification of Lignocellulosic Materials at short Residence Time", Energy from Biomass, Applied Science Publishers, pp. 548-553 (1981)
- [10] F. H. Holmes and C. J. G. Shaw, "The Pyrolysis of Cellulose and The Action of Flame-Retardants", J. Appl. Chem., 11, June (1961)



- [11] G. A. Byrne, D. Gardiner, and F. H. Holmes, "The Pyrolysis of Cellulose and The Action of Flame-Retardants", J. Appl. Chem., Vol 16, March (1966)
- [12] D. P. C. Fung, Yoshio Tsuchiya, and Kikuo Sumi, "Thermal Degradation of Cellulose and Levoglucosan The Effect of Inorganic Salts", Wood Science, 5, No. 1, July (1972)
- [13] Yoshil Tsuchiya and Kikuo Sumi, "Thermal Decomposition Products of Cellulose", Journal of Applied Polymer Science, Vol. 14, pp. 2003-2013 (1970)
- [14] S. L. Madorsky, V. E. Hart and S. Straus, "Pyrolysis of Cellulose in a Vacuum", J. Res. Natl. Bur., 56, (1956)
- [15] W. G. Parks, J. G. Erhardt, Jr., and D. R. Roberts, Amer. Dyestuff Reprtr. 294 (1950)
- [16] E. M. Suuberg, W. A. Peters, and J. B. Howard, "A Comparison of the Rapid Pyrolysis of a Lignite and a Bituminous Coal", Thermal Hydrocarbon Chemistry pp. 239, Advances in Chemistry Series No. 183, A. G. Obald, H. G. Davis, and R. T. Eddinger, Ed., Am. Chem. Soc., Washington, D. C. (1979)
- [17] J. E. Trautz, "The Flash Pyrolysis of Cellulose in the Presence of K_2CO_3 ", M. S. Thesis, Department of Chemical Engineering, Michigan State University, East Lansing (1985)
- [18] C. C. Sweeley, R. Bently, M. Makita and W. W. Wells, "Gas-Liquid Chromatography of Trimethylsilyl Derivatives of Sugars and Related Substances", J. Am. Chem. Soc., Vol. 85, 2497 (1963)
- [19] R. Pecina, G. Bonn, E. Burtscher, and O. Bobleter, "High-Performance Liquid Chromatographic Elution Behavior of Alcohols, Aldehydes, Ketones, Organic Acids and Carbohydrates on a Strong Cation-Exchange Stationary Phase", Journal of Chromatography 287 (1984)

APPENDIX

APPENDIX A

Power Requirements for Heating the Screen

Theoretical power requirement is total heat transfer by conduction, convection, and radiation.

1. Heat Flow by Conduction

$$\rho C_p \frac{\partial T}{\partial t} = (\nabla \cdot k \nabla T) \quad \text{----- (A-1)}$$

If the thermal conductivity (k) is independent on temperature or position, Eq. (A-1) becomes

$$\frac{\partial T}{\partial t} = \alpha \nabla^2 T \quad \text{----- (A-2)}$$

where α = thermal diffusivity ($\alpha = k/\rho C_p$)

ρ = fluid density

C_p = heat capacity

By dimensionless form of temperature, $\theta = (T - T_0)/(T_1 - T_0)$, the Eq. (A-2) for one dimension becomes

$$\frac{\partial \theta}{\partial t} = \frac{\partial^2 \theta}{\partial y^2} \quad \text{----- (A-3)}$$

I.C. : $t = 0$, $\theta = 0$ for all y

B.C.1 : at $y = 0$, $\frac{\partial \theta}{\partial y} = 1$ for all t

B.C.2 : at $y = \infty$, $\theta = 0$ for all t

The solution in Eq. (A-3) becomes

$$\theta = 1 - \frac{2}{\sqrt{\pi}} \int_0^{y/\sqrt{4\alpha t}} e^{-n^2} dn \quad \text{----- (A-4)}$$

$$\frac{T - T_0}{T_1 - T_0} = 1 - \operatorname{erf} \frac{y}{(4\alpha t)^{1/2}} \quad \text{----- (A-5)}$$



From the Fourier's law of heating conduction,

$$q_y = -kA \frac{\partial T}{\partial y} \quad \text{----- (A-6)}$$

From Eq. (A-5) and Eq. (A-6)

$$q_y|_{y=0} = \frac{kA}{\sqrt{\pi \alpha t}} (T_1 - T_0) \quad \text{----- (A-7)}$$

The properties for helium based on the arithmetic mean temperature $T_m = (T_1 + T_0)/2 = 385^\circ\text{C}$ are obtained from the Fundamentals of Momentum, Heat and Mass Transfer by Welty, Wicks, Wilson, second edition.

$$T_1 = 750^\circ\text{C} (1382^\circ\text{F}) \quad T_0 = 20^\circ\text{C} (68^\circ\text{F})$$

At 385°C (725°F), helium has the following properties.

$$\begin{aligned} \rho &= 4.6825 \times 10^{-3} \text{ [lb/ft}^3\text{]} & c_p &= 1.24 \text{ [Btu/lb }^\circ\text{F]} \\ k &= 0.1394 \text{ [Btu/hr ft }^\circ\text{F]} & \alpha &= 24.0084 \text{ [ft}^2\text{/hr]} \end{aligned}$$

Therefore,

$$q_y|_{y=0} = 27.825 \text{ [Btu/hr]} = 8.180 \text{ [Joule/s]}$$

2. Heat Flow by Convection

$$Gr = \frac{L^3 \rho^2 g \Delta T_0}{\mu^2} \quad \text{----- (A-8)}$$

$$L = 3.54 \text{ [cm]} \quad g = 980 \text{ [cm/s}^2\text{]}$$

$$\rho = 7.507 \times 10^{-5} \text{ [g/cm}^3\text{]} \quad \beta = 1.5198 \times 10^{-3} \text{ [1/K]}$$

$$\mu = 3.327 \times 10^{-4} \text{ [g/cm s]} \quad T_0 = 730 \text{ [K]}$$

$$Pr = 0.72125$$

$$Gr Pr = 1771.2$$

$$Nu = C (Gr Pr)^m$$

Even though the value $Gr Pr$ (1771.2) is not in the range

given in Table 7-1 in Heat Transfer by J. P. Holman, it is roughly applied to the two cases:

a) upper surface of heated plate

$$\text{Gr Pr} = 2 \times 10^4 \text{ -- } 8 \times 10^4 \quad C = 0.54 \quad m = 1/4$$

b) lower surface of heated plate

$$\text{Gr Pr} = 10^5 \text{ -- } 10^{11} \quad C = 0.58 \quad m = 1/5$$

From Eq. (A-9), $h = (k/L) C (\text{Gr Pr})^m$

where L = mean distance of the two dimension for rectangular surface

For upper surface of screen

$$h_{\text{up}} = 4.1937 [\text{Btu/ft}^2 \text{ hr } ^\circ\text{F}]$$

$$q_{\text{up}} = h A (T_1 - T_0) = 17.8109 [\text{Joule/s}]$$

For lower surface of screen

$$h_{\text{low}} = 3.0990 [\text{Btu/ft}^2 \text{ hr } ^\circ\text{F}]$$

$$q_{\text{low}} = h A (T_1 - T_0) = 13.1615 [\text{Joule/s}]$$

$$\begin{aligned} \text{Total heat flow by natural convection} &= q_{\text{up}} + q_{\text{low}} \\ &= 30.972 [\text{Joule/s}] \end{aligned}$$

3. Heat Flow by Radiation

$$q_{12} = A_1 F_{12} (T_1^4 - T_2^4) \text{ ----- (A-10)}$$

$$F_{12} = \left(\frac{1}{\epsilon_1} + \frac{A_1}{A_2} \left(\frac{1}{\epsilon_2} - 1 \right) \right)^{-1} \text{ ----- (A-11)}$$

F_{12} = shape factor

A_1 = surface area of the screen

$$= 2 \times 2 \times 2.54 [\text{cm}^2] = 3.150 [\text{in}^2]$$

A_2 = area of aluminum foil wrapping inside the tube



$$= 2 \times 0.75 \times 3 \text{ [in}^2\text{]} = 14.137 \text{ [in}^2\text{]}$$

$$\epsilon_1 = \text{emissivity of the screen} = 0.6$$

$$\epsilon_2 = \text{emissivity of aluminum foil} = 0.52$$

$$T_1 = \text{temperature of screen} = 1023 \text{ [K]}$$

$$T_2 = \text{temperature of ceramic tube} = 293 \text{ [K]}$$

$$\text{Therefore, } F_{12} = 0.5341$$

$$q_{\text{rad}} = 67.013 \text{ [Joule/s]}$$

$$\begin{aligned} \text{Thus, total heat flow } q_{\text{total}} &= q_{\text{cond}} + q_{\text{conv}} + q_{\text{rad}} \\ &= 8.180 + 31.972 + 67.013 \\ &= 106.165 \text{ [Joule/s]} \end{aligned}$$

The actual power requirement is calculated from the values of voltage and current observed in the experiment.

$$\begin{aligned} \text{Power [Joule/s]} &= \text{Current [A]} \times \text{Voltage [V]} \\ &= 36 \text{ [A]} \times 8.5 \text{ [V]} = 306 \text{ [Joule/s]} \end{aligned}$$

Comparison between the actual and theoretical power requirement shows that the actual power requirement is much larger. The reasons are as follows. First, the heat loss through the copper electrodes was not included in the calculation. Second, the heat flow was calculated on the basis of steady state screen temperature (750°C) though heat flow is varied by heating rate. Third, some of properties (emissivities) were roughly used to calculate heat flow.

The following Figures 11 (a-f) show the relation between power (number on dial in Electron Arc Division Power Supply), heating rate, and peak temperature. In

these Figures, chart speed is 5 in/min.



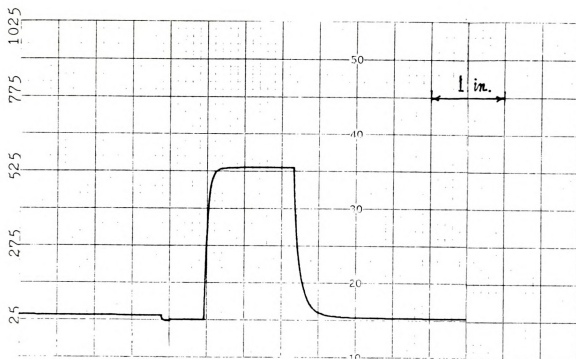


Figure 11-a. Peak temperature at 600°C set point temperature, 10 on dial in Electron Arc Division Power Supply.

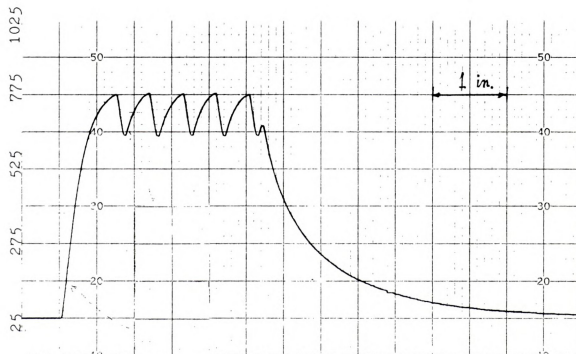


Figure 11-b. Peak temperature at 750°C set point temperature, 15 on dial in Electron Arc Division Power Supply.



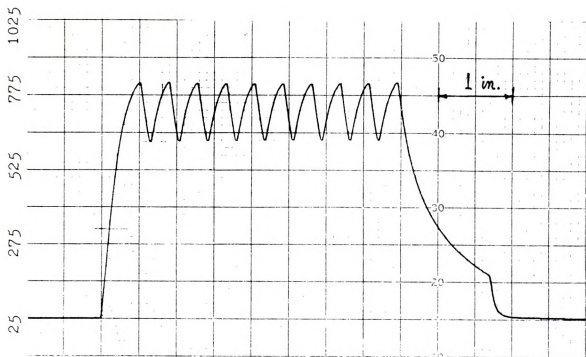


Figure 11-c. Peak temperature at 750°C set point temperature, 17 on dial in Electron Arc Division Power Supply.

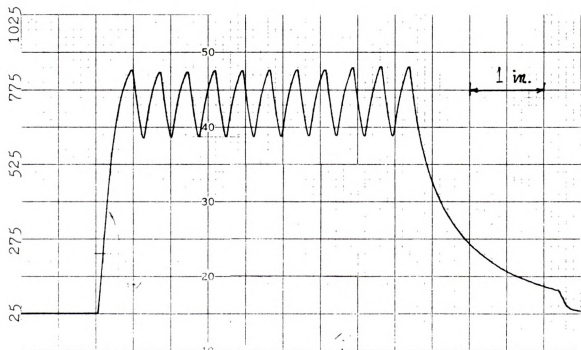


Figure 11-d. Peak temperature at 750°C set point temperature, 18 on dial Electron Arc Division Power Supply.



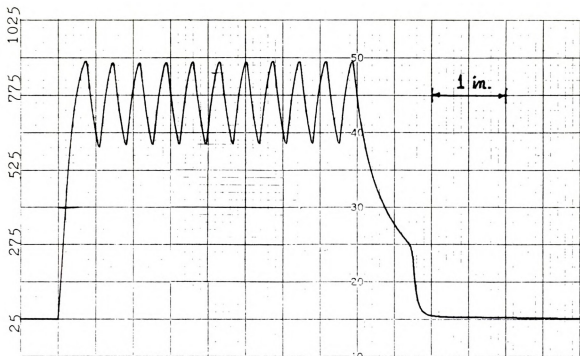


Figure 11-e. Peak temperature at 750°C set point temperature, 20 on dial in Electron Arc Division Power Supply.

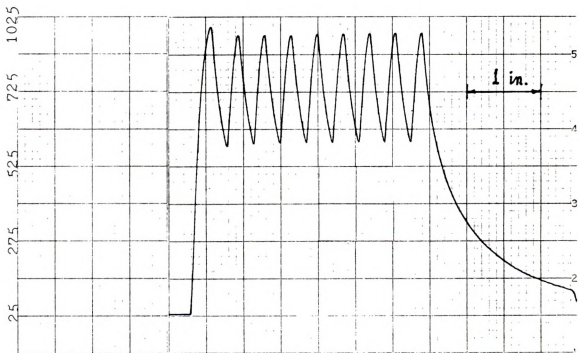


Figure 11-f. Peak temperature at 750°C set point temperature, 24 on dial in Electron Arc Division Power Supply.

APPENDIX B
WATER CALIBRATION

As shown in Section D in CHAPTER III, G.C. and two traps (17) and (21) are prepared to collect H_2O by placing the trap (20) in liquid nitrogen around, the trap (17) in dry ice / acetone.

After 5 minutes, the 3-Way Whitey Valve (8) is changed to route (a), where the line is disconnected to inject H_2O . Distillated water (2 microliter) is injected into the 3-Way Whitey Valve (8) using a 10 microliter Hamilton Syringe. The 3-Way Whitey Valve is changed to the "close" position and the reactor without sample is heated to $750^{\circ}C$ for 45 seconds, Helium is then purged into the reactor and through two loops (17) and (21) by changing the 3-Way Whitey Valve (8) into route (b).

After 25 minutes, the 3-Way Whitey Ball Valve (18) and (19) are changed to route (c) to isolate the collected water in the loop (20). The Model XKR Sargent-Welch Record and Integrate are adjusted to the "pen" position as the some way as the procedure of gas calibration in CHAPTER III.

The analysis of H_2O by G.C. is exactly the same as described in Section C in CHAPTER III. Figure 12 resulted from the water calibration.

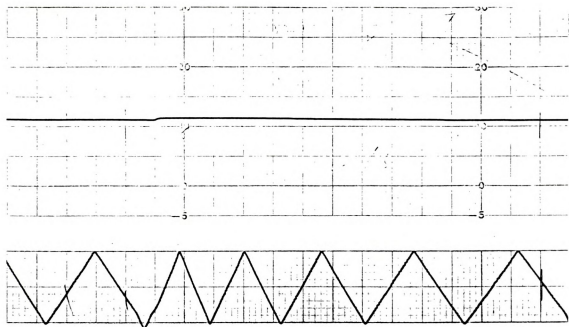


Figure 12-a(1). Chromatogram of water without loading water (liquid nitrogen trap (20))

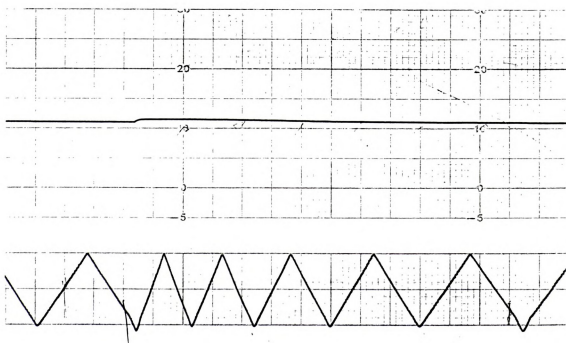


Figure 12-a(2). Chromatogram of water without loading water (dry ice/acetone trap (17))

PRINTED IN U.S.A.

SARGENT-WELCH SCIENTIFIC COMPANY

c

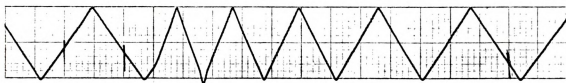
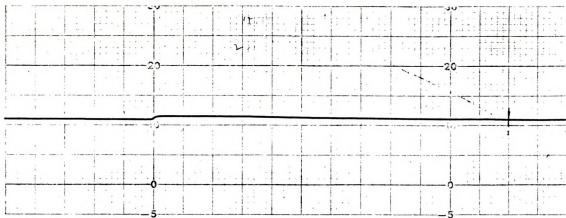


Figure 12-b(1). Chromatogram of 4 μ l distilled water
(liquid nitrogen trap (20))

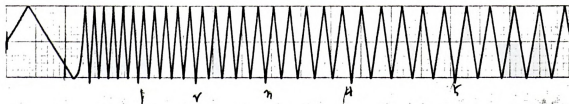
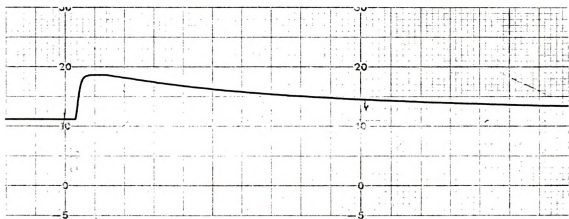


Figure 12-b(2). Chromatogram of 4 μ l distilled water
(dry ice/acetone trap (17))

SARGENT-WELCH SCIENTIFIC COMPANY

CATALOG NO. S-72164

APPENDIX C

CHROMATOGRAM OF PYROLYSIS GASES AND RAW DATA

Figure 13 is the chromatogram of pyrolysis gases (CO , CH_4 , CO_2 , H_2O , C_2H_4) at 650°C set point temperature, 15 mm Hg helium. The chart speed is 2 cm/min and attenuation is 32. Figure 14 is the chromatogram of pyrolysis (H_2) using Hydrogen Transfer System. The chart speed is 2 cm/min and attenuation is 4. Figure 15 is the chromatogram of pyrolysis (H_2O) obtained from the dry ice / acetone trap (17). The chart speed and attenuation are the same as those in Figure 13.

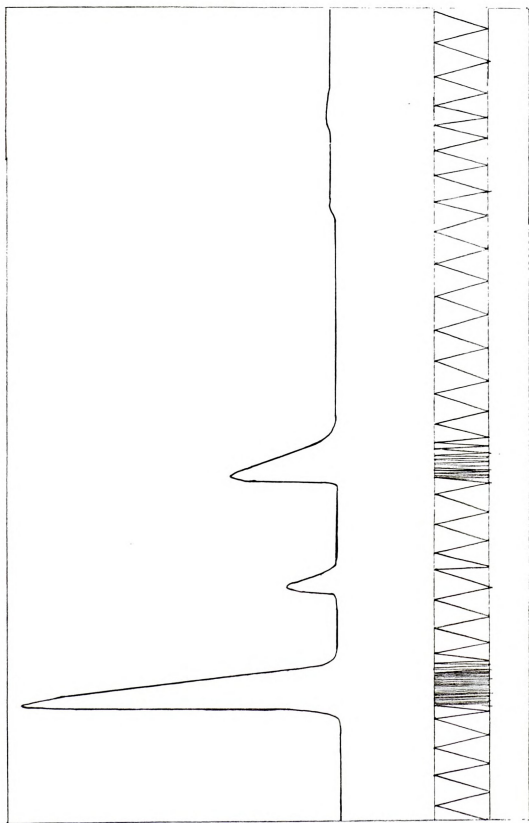


Figure 13. Chromatogram of Pyrolysis Gases
(CO, CH₄, CO₂, H₂O, C₂H₄)

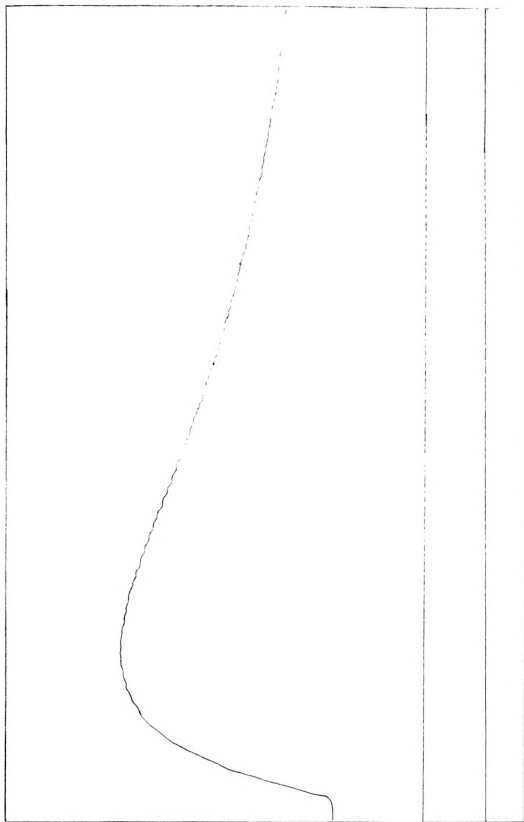


Figure 14. Chromatogram of Pyrolysis Gas (H_2)

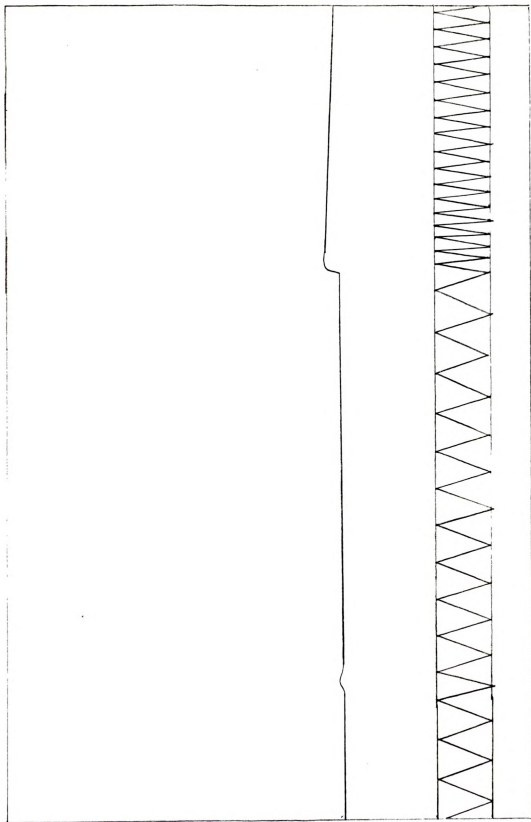


Figure 15. Chromatogram of Pyrolysis Gas (H_2O)

0%

15 min, set pt temp 650°C

	before	after	Δ	Σ
Al. foil				
reactor	0.5396	0.5444	0.0048	} 0.007 tan
circuit	0.1264	0.1270	0.0006	
electrode	0.1421	0.1426	0.0005	} 0.0013 chan
screen	0.7630	0.7633	0.0003	
cellular	0.0136			

tan wt % \rightarrow 43.38 %chan \rightarrow 2.21 %

gases ;

	cali.	pyrolysis	gas.
CO	23.52	307.07	
CH ₄	20.87	13.70	
CO ₂	29.28	81.27	
H ₂	148.74 (atan 64)	205.13 (atan 6)	
H ₂ O		162.39	
C ₂ H ₄	122.25	7.92	

1 x, 16.00g, set pt. temp = 760°C 1 atm.

sample # 22 is used

& same sample gas calibration as before

	before	after	Δ		
aluminum foil	reactor	0.3987	0.8004	0.0017	$\left\{ \begin{array}{l} \text{tan} \\ = 0.002 \end{array} \right.$
	viscint	0.1258	0.1261	0.0004	
	electrode	0.1211	0.0011	0.0000	
	screen	0.9753			
	draw cellular	0.0014	0.0014	(separable for screen)	

of counts

calibration

pyrolysis gas

CO	23.2375	457.25
CH ₄	~0.9875	83.6625
CO ₂	26.99275	178.1
H ₂	154.794573 (atom 64)	2807.025 (atom 4)
H ₂ O		315.25
CO ₂	122.25	28.778

Water Calibration.

Procedure :

1. measure flow rate 30 ml/min
 2. turn on switch (2)
 3. put hot water at the bottom of N_2 trap after setting $175^\circ C$
 4. After arriving $175^\circ C$, take hot water away from N_2 trap and change hot water to dry. N_2 at the bottom.
Wait 5 minutes
 5. Close dry N_2 trap
 6. change 6-port valve to "Reactor through Loop"
 7. measure flow rate for 5 minutes
 8. Put dry. N_2 and dry ice/acetone at each trap, but N_2 trap still closed. Wait 25 minutes
 9. Open N_2 trap.
 10. Change dry ice trap valve to vent position in order to inject distilled water, then inject.
 11. Wait 5 minutes
 12. Close dry ice trap and heat up to $75^\circ C$ in reactor
 13. Wait 4 minutes
 14. Purge He for 25 minutes
 15. Close N_2 trap valve and change 6-port valve to "6-c through Loop", then put hot water at N_2
 16. Wait 2 minutes, then ramp $175^\circ C$
- When temp. arrives at $175^\circ C$
1. Turn blower position and close N_2 trap, then turn 6-port valve
 2. Put dry. N_2 at N_2 trap and put hot water at dry ice trap.
 3. Wait about 25 minutes, then close N_2 trap and turn 6-port valve.
 4. Put hot water at N_2 trap.
 5. same.





MICHIGAN STATE UNIVERSITY LIBRARIES



3 1293 03062 2603